MATHEMATICAL MODELS, ANALYSES, AND SIMULATIONS OF THE SPREAD OF DISEASE

by

JANICE MOORE

A dissertation submitted in partial fulfillment of the
requirements for the degree of

DOCTOR OF PHILOSOPHY IN APPLIED MATHEMATICAL SCIENCES

2026

Oakland University
Rochester, Michigan

Doctoral Advisory Committee:

Meir Shillor, Ph.D., Chair
Anna Spagnuolo, Ph.D.
Darrell Schmidt, Ph.D.
Eddie Cheng, Ph.D.

I dedicate this to my husband, Chad, who took on as much work as I did in this endeavor and never wavered in his support.

ACKNOWLEDGMENTS

This work would not have been possible without the efforts and support of my doctoral advisory committee chair, Dr. Meir Shillor. After completing my master's degree, you predicted I would return to pursue my doctorate. The idea stayed with me until I could no longer ignore it. It has been an honor to work with you, and I am beyond grateful for all you have taught me.

I am also extremely grateful to my doctoral advisory committee, Dr. Eddie Cheng, Dr. Darrell Schmidt, and Dr. Anna Spagnuolo.

Janice Moore

ABSTRACT

MATHEMATICAL MODELS, ANALYSES, AND SIMULATIONS OF THE SPREAD OF DISEASE

by

Janice Moore

Adviser: Meir Shillor, Ph.D.

Models in mathematical biology have been evolving for centuries and have had a significant impact on our understanding of biological processes. This work includes three new models. We present an extension of the SIR (Susceptible-Infected-Recovered) model, which allows hospitalization rates and infection rates to vary with time as system variables, and we present two cancer treatment models. The first of the two cancer treatment models explores the effects of combining chemotherapy and immunotherapy in the treatment of a tumor. The second cancer treatment model considers the combination of chemotherapy, immunotherapy, and virotherapy in the treatment of a tumor. For each of these models, we establish that they are positive invariant and bounded, prove that a stable solution exists, and use numerical methods to explore the behavior of the solutions. Each model produced results that encourage further study. Thus, this work is a contribution to the discipline of mathematical epidemiology.

TABLE OF CONTENTS

TABLE OF CONTENTS—Continued

LIST OF TABLES

LIST OF FIGURES

CHAPTER ONE

Introduction

This dissertation presents three novel models in the field of mathematical epidemiology. The first extends the standard SIR model by assuming that hospitalization and infection rates vary with time as system variables. The second and third models are related to cancer treatment. They are designed to model the impact of combinations of treatments on a cancer tumor. The first of these models considers a combination of chemotherapy and immunotherapy. The second is an extension of the first and considers the impact of a combination of chemotherapy, immunotherapy, and virotherapy. This work contributes to the discipline of mathematical epidemiology.

The broader topic of mathematical biology, which is the foundation of mathematical epidemiology, dates back to 1202 with Leonardo di Pisa. He included an exercise in his textbook, *Liber Abbaci*, which considered the population growth of rabbits when you start with two immature rabbits [29]. From those humble beginnings, mathematical biology has evolved into its own field with numerous subfields of its own. By the mid to late 1900's there were works relating mathematics to nerve conduction and excitation [1], the behavior of reacting and diffusing chemicals in a bounded domain [3], enzyme kinetics [27], ecology [24], [25], and epidemiology [24], [25], to name a few.

Presently, the literature on mathematical epidemiology is extensive, including [19], [22], and others cited throughout this work, which is comprised of three original epidemiological models. These types of models have their foundations in continuous population models for single species, which have the following general

form. Let $N(t)$ be the population of the species at time t, then the rate of change

$$\frac{dN}{dt} = \text{births} - \text{deaths} + \text{migration},$$

is a conservation equation for the population. The simplest of these would be a population without migration. Thus, the equation becomes

$$\frac{dN}{dt} = bN - dN,$$

where b is the birth rate and d is the death rate. Consequently, we have

$$N(t) = N_0 e^{(b-d)t},$$

where N_0 is the initial population. The population grows exponentially when $b > d$ and decreases exponentially when $b < d$. Another, more complex, but realistic model is the logistic model proposed by Verhulst [28]:

$$\frac{dN}{dt} = rN(1 - \alpha N),$$

where r and α are positive constants. Specifically, r is the growth rate of N, and α is the reciprocal of the carrying capacity of the habitat. The solution is given by

$$N(t) = \frac{N_0 e^{rt}}{1 + \alpha N_0 (e^{rt} - 1)},$$

which is such that $N(0) = N_0$ and $N \to 1/\alpha$ as $t \to \infty$.

There is also often a harvesting term in such equations. This term represents the loss of the population due to harvesting. This term fits into the population model as follows

$$\frac{dN}{dt} = rN\left(1 - \alpha N\right) - \gamma N,$$

where γ is a positive constant. So the loss due to harvesting is linearly proportional to the population.

Beyond the dynamics of a single population in isolation, we must consider the impact that other populations have on the population under study. Volterra first proposed a model that addressed this interaction in his 'predator-prey' model.

$$\frac{dN}{dt} = aN - bPN,$$
$$\frac{dP}{dt} = cNP - dP.$$

In this model $N(t)$ represents the prey population and $P(t)$ represents the predator population. In the prey equation, the prey is allowed to grow unbounded at a rate of a. The term $-bNP$ is the one of interest for our purposes. The prey's growth rate is decreased by a term proportional to the predator and prey populations. Similarly, since the prey is beneficial to the predator population, its growth rate is increasing by cNP, a term again proportional to both populations.

Another term that arises in one of our models is the Michaelis-Menten term, which originated in the study of chemical reaction kinetics,

$$v = \frac{V[A]}{K_{mA} + [A],}$$

where v is the rate of reaction, V is the limiting rate, K_{mA} is the substrate concentration at which $v = 0.5V$, and $[A]$ is the concentration of the reactant [33]. When used to describe the rate of change of a population, the population size follows a path similar to the top half of a logistic curve, which can be used to describe populations that grow quickly from the start and have an upper limit, similar to the carrying capacity.

We use the terms described above as the basis for the models in Chapters 4 and 5. For Chapter 3, we build upon the family of SIR models. SIR models originated with Kermack-McKendrick [22]. In their model, SIR represents the Susceptible, Infective, and Removed populations. This is a compartmentalized

model in which each population grows from specific sources and depletes to specific destinations. In other words, in this simplest example, there is a susceptible population S. Members of this population, either remain susceptible, staying in the S compartment, or become infected and move to the I compartment. The infective population I is generated from the susceptible population that becomes infected. The infectives remain in that population until they either get healthy or die and are thus removed from the infective population and enter the removed compartment R. This type of model is typically represented as

$$S \to I \to R.$$

The system of equations associated with this particular example is

$$\frac{dS}{dt} = -rSI,$$
$$\frac{dI}{dt} = rSI - aI,$$
$$\frac{dR}{dt} = aI.$$

The terms in this system make it clear where each population is going. The loss rate of the susceptibles, rSI is the gain by the infectives. Likewise, the loss rate of the infectives, aI is gained by the removed. This orignal model spawned countless modified versions to describe a wide range of diseases. For our SIR-type model, we considered a general disease where susceptibles who become infected are either hospitalized with a severe case of the illness or stay at home with a mild form. We were curious what effect it would have on the system if the infection rate of the disease, as well as the hospitalization rate were allowed to vary with time, which we analyze in Chapter 3. In Chapters 4 and 5 we use the fundamentals of modeling epidemiological scenarios to create a model for the effects of chemotherapy and

immunotherapy on a tumor (Chapter 4) and the effects of chemotherapy, immunotherapy, and virotherapy on a tumor (Chapter 5).

In each of these three chapters, we present briefly the background for the model and the related mathematical problem, some relevant literature on the model, and motivation for considering it. We then present the model in detail and establish the boundedness, positivity, and existence of global solutions. The stability of the disease-free equilibrium (DFE) points and of the endemic equilibrium points (EE) are studied, indicating whether the disease will eventually vanish or will persist in the population. Then we describe a numerical method for the computer approximations of the solutions used to create the simulations. We present simulations related to a typical scenario, as well as those that produce interesting solutions. The conclusions for each model and some opportunities for further study are also described in each chapter.

This dissertation is a contribution to the rapidly expanding literature on the applications of mathematics, dynamical systems in particular, to predictive epidemiology. Indeed, the modified SIR model adds various processes to the basic SIR model, with the aim of providing the community with tools to improve the outcome of disease prediction and treatments. This model includes the observed phenomena of diseases evolving through a population and may be instructive as to the effects of this evolution, potentially leading to better treatment response. In terms of the cancer treatment models, studies indicate that combining therapies may be beneficial. Our models may be useful in revealing combinations of treatments that warrant exploration and may even be helpful in determining optimal treatment schedules.

CHAPTER TWO

Mathematical Preliminaries

For a mathematical epidemiological model to be feasible, it must meet certain criteria. It is necessary for a global solution to exist, and all solutions must be nonnegative and bounded. It is then important to understand the stability of the system. Depending on the purpose of the model, this may involve analysis of the disease free equilibrium and/or the endemic equilibrium conditions. This chapter provides an overview of techniques and strategies employed in the theory of dynamical systems to establish the existence, uniqueness, positivity, boundedness, and stability of biological models in general, as well as the numerical methods employed to approximate the solutions. These techniques and strategies will be implemented in Chapters 3, 4, and 5.

2.1 Nonnegativity and Boundedness of Solutions

Each model in this paper is a nonlinear, nonhomogeneous, nonautonomous system of first order differential equations. Each of these equations is Lipschitz continuous.

In order to show that the variables in our models are nonnegative or positive, we create inequalities from each of the equations in the system. For example, in Chapter 3 our first equation in the model is

$$\frac{dS}{dt} = P - (\beta I_m + \epsilon_h \beta I_h)\frac{S}{N} - \mu S + \rho R.$$

As long as S_0, I_{m_0}, I_{h_0}, and R_0 are all greater than zero, then there exists an interval $[0, T]$ such that S, I_m, I_h, and R are all greater than zero, since they are

continuous functions. This guarantees that

$$\frac{dS}{dt} \geq -(\beta I_m + \epsilon_h \beta I_h)\frac{S}{N} - \mu S.$$

From here we can use separation of variables to establish that $S > 0$. All of the other equations in the three models are addressed similarly to show that each variable is nonnegative, when the initial conditions are nonnegative.

Boundedness can be determined following a similar strategy. In the case of the SIR model in Chapter 3, we can add the first four equations of the model together to establish an upper bound on the total population, which is an upper bound on all of the other population subgroups. In Chapters 4 and 5, we set up inequalities similar to those set up to show nonnegativity. For example, the first equation in the model in Chapter 4 is

$$\frac{dH}{dt} = \alpha_1 H(1 - \alpha_H H) - \gamma_1 KH - \mu_1 DH - \mu_H H,$$

which implies that

$$\frac{dH}{dt} \leq \alpha_1 H(1 - \alpha_H H).$$

Again, using separation of variables, we can establish an upper bound on H, and can similarly bound all of the variables in the three models.

2.2 Existence and Uniqueness of Solutions

In order to prove the existence of a local solution in each of the three models, we follow the structure outlined by DiPrima and Boyce [4] for general systems of

first order differential equations. Given the system

$$\begin{aligned} x_1' &= F_1(t, x_1, x_2, ..., x_n), \\ x_2' &= F_2(t, x_1, x_2, ..., x_n), \\ &\vdots \\ x_n' &= F_n(t, x_1, x_2, ..., x_n) \end{aligned} \tag{2.1}$$

and initial conditions

$$x_1(t_0) = x_1^0, \quad x_2(t_0) = x_2^0, \quad ..., \quad x_n(t_0) = x_n^0, \tag{2.2}$$

we can apply Theorem 2.2.1.

Theorem 2.2.1. *Existence and uniqueness of a local solution on an interval*

Let each of the functions $F_1, ..., F_n$ and the partial derivatives $\partial F_1/\partial x_1, ..., \partial F_1/\partial x_n, ..., \partial F_n/\partial x_1, ..., \partial F_n/\partial x_n$ be continuous in a region R of $tx_1x_2...x_n$ space defined by $\alpha < t < \beta$, $\alpha_1 < x_1 < \beta_1$, ..., $\alpha_n < x_n < \beta_n$, and let the point $(t_0, x_1^0, x_2^0, ..., x_n^0)$ be in R. Then, there is an interval $|t - t_0| < h$ in which there exists a unique solution $x_1 = \phi_1(t), ..., x_n = \phi_n(t)$ of the system of differential equations (2.1) that also satisfies the initial conditions (2.2).

In order to prove the global existence of a unique solution in each of the three models, we refer to Caraballo and Han [6]. We let
$f : (a, +\infty) \times \mathbf{R}^d \subseteq \mathbf{R}^{d+1} \to \mathbf{R}^d$ be a continuous mapping, and let (t_0, x_0) be a point in $(a, +\infty) \times \mathbf{R}^d$. Then we can formulate the following initial value problem

$$\frac{dx(t)}{dt} = f(t, x), \quad x(t_0) = x_0 \tag{2.3}$$

Theorem 2.2.2. *Assume that $f : (a, +\infty) \times \mathbf{R^d} \to \mathbf{R}^d$ is continuously differentiable, i.e., its partial derivatives of first order are continuous functions, and*

there exist non-negative continuous mappings $h, k : (a, +\infty) \to \mathbf{R}$ *such that*

$$|f(t,x)| \leq h(t)|x| + k(t), \text{ for all } (t,x) \in (a,+\infty) \times \mathbf{R}^d.$$

Then, there exists a unique solution to (2.3) which is defined globally in time.

Since we establish that all of the variables are bounded in each of our models, we have that each of our systems of differential equations is bounded, and consequently, we are guaranteed a unique global solution for each model.

2.3 Stability

To assess the stability of our models, we can use the Jacobian matrix, as shown by Goode and Annin [18]

$$J(x_1, x_2, ..., x_n) = \begin{bmatrix} \frac{\partial F_1}{\partial x_1} & \cdots & \frac{\partial F_1}{\partial x_n} \\ \vdots & \vdots & \vdots \\ \frac{\partial F_n}{\partial x_1} & \cdots & \frac{\partial F_n}{\partial x_n} \end{bmatrix}.$$

The Jacobian provides a linear approximation of the system at an equilibrium point $(x_1^0, x_2^0, ..., x_n^0)$ as

$$u' = J(x_1^0, ..., x_n^0)u,$$

where

$$u = \begin{bmatrix} x_1 - x_1^0 \\ \vdots \\ x_n - x_n^0 \end{bmatrix}.$$

Near the equilibrium point, the behavior of the trajectories to the nonlinear system is closely approximated by the trajectories of the corresponding linear system (except for the cases of a center). Therefore, we need only show that the eigenvalues of the Jacobian matrix at the equilibrium point have a negative real part or

determine the conditions under which they have a negative real part. This also excludes the center equilibrium points which have eigenvalues with zero real part.

2.4 Numerical Methods and Simulations

Very often systems of ordinary differential equations cannot be solved explicitly, in closed form, so we must rely on numerical methods to obtain accurate approximations of the solution. Two such numerical methods were applied to our models. For the modified SIR model in Chapter 3 and the model for Chemotherapy and Immunotherapy of a Cancer Tumor in Chapter 4, Euler's Method was found to be sufficient. The model for Chemotherapy, Immunotherapy, and Virotherapy of a Cancer Tumor in Chapter 5 required a more sophisticated approximation method. We used the explicit Runge-Kutta (4,5) formula, the Dormand-Prince pair, via MATLAB's ode45 function.

Both methods are discrete variable methods which can be used to obtain an accurate approximation to the solution of an initial value problem. These methods involve an iterative process that finds a sequence of points (t_k, x_k) that approximates $(t_k, x(t_k))$ along the graph of a solution of the first-order differential equation $x' = f(t, x)$. Letting $t_0 = 0$ and $x(0) = x_0$, we begin with an initial value $(0, x_0)$. Then, using a step size Δt, we can approximate the next value in the solution x at t_{k+1}

$$t_{k+1} = t_k + \Delta t.$$

For Euler's method, we move Δt time units along the straight line generated by the slope field at the point (t_k, x_k) [20]. Since the slope at this point is $x'(t_k, x_k) = f(t_k, x_k)$, we use the equation

$$x_{k+1} = x_k + f(t_k, x_k)\Delta t.$$

In the simulations that used Euler's method, we set up an algorithm in MATLAB to complete this calculation for all the equations in our model and plotted the approximated solutions.

The Dormand-Prince algorithm is in the Runge-Kutta method family. For context, the (Fourth-order) Runge-Kutta method requires four slopes, m_k, n_k, p_k, and q_k. Like Euler's method, we move along a straight line from (t_k, x_k) to (t_{k+1}, x_{k+1}). In this case, the slope of this line,

$$x_{k+1} = x_k + \left(\frac{m_k + 2n_k + 2p_k + q_k}{6}\right)\Delta t,$$

is a weighted average of the four slopes, where

$$m_k = f(t_k, x_k),$$

$$n_k = f(t_k + \frac{\Delta t}{2}, y_k), \text{ where } y_k = x_k + m_k\frac{\Delta t}{2},$$

$$p_k = f(t_k + \frac{\Delta t}{2}, z_k), \text{ where } z_k = x_k + n_k\frac{\Delta t}{2},$$

$$q_k = f(t_{k+1}, w_k), \text{ where } w_k = x_k + p_k\Delta t.$$

The Dormand-Prince algorithm is an extension of this. For the Dormand-Prince algorithm, six functions are used to simultaneously solve fourth order and fifth order Runge-Kutta updates. If the difference between these updates is above a prescribed tolerance, the time increment Δt_k will be decreased and the updates are recalculated [8]. Our model for Chemotherapy, Immunotherapy and Virotherapy of a Cancer Tumor was too complex for Euler's method. It required the efficiency of the Dormand-Prince Algorithm.

CHAPTER THREE

A Modified SIR Model with Dependent Infection and Hospitalization Rates

3.1 Background

In this chapter, we follow [26] (on which it is based), we develop, analyze, and computationally simulate a new, extended version of the SIR model. In this model, we allow two measures of the severity of the disease to vary within the system. The infected population is divided into those who have mild symptoms and those who have a severe case requiring hospitalization. This hospitalization rate is denoted α^*. The rate of infection of the disease β is also allowed to vary with time, rather than assumed constant. This allows for the observed behavior of many diseases, including COVID-19. The rate equations for both variables are linear in the populations. This is done for simplicity, though it is likely that the relationships are much more complex. Such relationships will most likely need to be determined for each disease separately. This model is meant to serve as an avenue to begin to represent how changes within a disease over time affect the overall progression of the disease. The concept of system-dependent infectivity was already considered in [7]. The approach here is quite general, intended as a foundation and not for specific applications.

Infectious diseases are a major cause of suffering, morbidity, and mortality worldwide. In an effort to minimize the impact of an infectious disease, epidemiologists must both understand the causes of the disease and be able to predict its progression. To this end, mathematical models were developed as early as 1906. Public health physicians including William Hamer and Ronald Ross laid the foundations for compartmentalized models. Hamer proposed that the spread of infection should depend on the number of susceptible individuals and the number of

infective individuals. This idea led to compartmental models, the most basic of which is the SIR model. Ross introduced the basic reproduction number in his study of eradicating malaria by reducing, rather than eliminating the population of mosquitos [5]. The number, variety, and complexity of compartmental models have grown extensively since then. Herbert W. Hethcote was one of the major contributors to the development of these types of models from 1970 until 2009. His most cited work is "The Mathematics of Infectious Diseases" [19], which describes how to build a mathematical, compartmental, epidemiological model and analyzes how to obtain the basic reproduction number, R_0, the contact number, σ, and the replacement number R. Some compartmentalized models are very general and designed to understand the behavior of a disease or diseases qualitatively. Others are more detailed and specific, with the purpose of making quantitative predictions on the behavior of a particular disease. Our model is of the general variety with the intent of understanding the impact of varying infection rates and hospitalization rates on the progression of a rather general disease over time.

The model is presented in the following section, where we also explain the equations for infectivity β and the rate of hospitalization α^*. The model consists of six differential equations for the four populations: susceptibles, mildly infected, hospitalized, and recovered, and the two rates. Following the presentation of the model, we perform an analysis to prove that the populations predicted by the model are nonnegative and bounded, which leads to the existence of a solution to the model. Once this is established, we use the Jacobian matrix to determine the stability of the disease-free equilibrium (DFE). The basic stability number, R_0, is also presented and shown to be below 1, indicating that the disease is declining, and will most likely die out. We use the ideas of Diekman et. al. [13] to compute R_0, using the reduced system that includes only the infection states. Following the

analysis of the DFE, we describe the conditions required for the existence of the endemic equilibrium (EE). Simulations are provided using an explicit time-stepping scheme. A variety of conditions are simulated to demonstrate the capabilities of the model.

3.2 The Model

As stated previously, this model is a modified SIR model of disease transmission that extends the typical model to include dependent rates of infection and hospitalization. This model assumes a generic disease in a large city, in which the disease is spreading. We use whole populations, do not consider their spatial spread, and assume that the populations are large enough to justify the use of a continuous description using ordinary differential equations (ODEs). The four populations considered in the model are susceptibles S, those who are healthy and can become infected; I_h, those infected severely enough to require hospitalization; I_m, those who are infected, but mildly enough to remain out of the hospital and recover at home; and R, recovered . These populations are functions of time, which is measured in days. The rate of change of each population is described below. We also assume that the rate of infection β and the disease severity function α^* are both dependent variables. This is the novelty of this work. The value of β is the probability that one susceptible person who comes in contact with an infected person becomes infected, while α^* is the fraction of those needing hospitalization. The compartmental structure of the model is shown below.

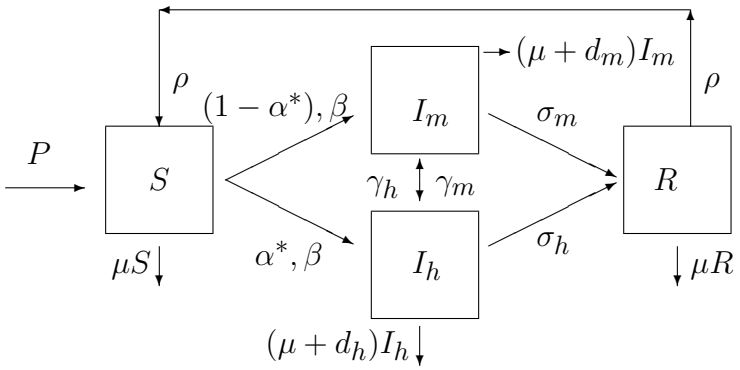

Figure 3.1: Compartmental structure and flow chart; β, the infection rate, and α^*, the fraction of hospitalized individuals, are also dependent variables

The susceptible population $S(t)$ consists of all the individuals who are alive and are not in another group. The net number of individuals who are added to the city per day by birth or arrive from the outside are denoted $P(t)$, and they add directly into $S(t)$. Individuals who leave this group are those who become infected or those who die from causes unrelated to the disease ("natural causes"). The death rate in the absence of the disease is denoted μ $(1/day)$. Individuals that leave S due to infection are separated into two groups, the mild cases and the severe cases. The mild cases I_m are those individuals who have contracted the disease but do not require hospitalization. The severe cases I_h are those individuals who require hospitalization due to the severity of the disease. The probability that one contact between a susceptible individual and a mildly infected individual results in infection is $\beta(t)$ $(1/day)$, the probability that one contact between a susceptible individual and an individual hospitalized due to the disease results in infection is $\epsilon_h\beta(t)$ $(1/day)$, where $\epsilon_h > 0$, is a correction factor, since although interactions between susceptibles and hospitalized individuals are limited, they may be more or less

infectious. We denote by $\alpha^* = \alpha^*(t)$ $(0 \leq \alpha^* \leq 1)$ the fraction of those infected who require hospitalization, and $1 - \alpha^*$ is the fraction of those infected who only have a mild infection.

There is a possibility that an individual has a mild case that develops into something severe enough to require hospitalization. Conversely, it is possible that an individual who required hospitalization initially recovers enough to complete their full recovery at home. These rates of transfer from one infected group to another are denoted by γ_h and γ_m. The number of individuals who move from I_m to I_h (per day) is $\gamma_m I_m$. The number of individuals who move from I_h to I_m (per day) is $\gamma_h I_h$

Both infected populations have death rates that take the disease into consideration. The death rates in I_m and I_h are $\mu + d_m$ $(1/day)$ and $\mu + d_h$ $(1/day)$ respectively. Individuals recover from the disease at a rate of σ_m for mild cases and σ_h for severe cases. Those in the recovered population become susceptible again at a rate of ρ.

The equations for β and α^* are likely to be of the general form

$$\frac{d\beta}{dt} = \Psi_\beta(I_m, I_h, R, \beta, \alpha^*), \qquad \frac{d\alpha^*}{dt} = \Psi_*(I_m, I_h, R, \beta, \alpha^*), \tag{3.1}$$

for given functions Ψ_β and Ψ_*, which would need to be found for each disease. We assume the infectivity of the disease increases with the number of infected, I_m, I_h, as the disease vector has more options to mutate, and it decreases with the number of recovered, as more individuals are immune. As noted below, we assume it is a relationship that is linear in the populations, which is probably a severe restriction. These functions require further investigation.

Since β and α^* are dependent variables, we must make sure that they stay within reasonable bounds. Let $0 < \beta_- < \beta_+$ and $0 \leq \alpha_- < \alpha_+ \leq 1$ be the limits for the allowed values of β and α^*, respectively. The restriction operators Φ_β, Φ_* acting

on $s \in \mathbf{R}$, as defined below, are introduced to guarantee that

$$\beta(t) \in [\beta_-, \beta_+], \qquad \alpha^*(t) \in [\alpha_-, \alpha_+]. \tag{3.2}$$

$$\Phi_\beta(s) = \begin{cases} \beta_-, & s \le \beta_-, \\ s, & \beta_- < s < \beta_+, \\ \beta_+ & s \ge \beta_+, \end{cases} \qquad \Phi_*(s) = \begin{cases} \alpha_-, & s \le \alpha_-, \\ s, & \alpha_- < s < \alpha_+, \\ \alpha_+ & s \ge \alpha_+. \end{cases} \tag{3.3}$$

Both operators are piecewise linear and Lipschitz continuous.

The total living population at time t is given by

$$N(t) = S(t) + I_m(t) + I_h(t) + R(t), \tag{3.4}$$

and is not assumed to be constant.

These assumptions lead to the following mathematical model for the dynamics of the disease with varying infection and hospitalization rates.

Model 3.2.1. *Find six functions* $(S, I_m, I_h, R, \widetilde{\beta}, \widetilde{\alpha^*})$*, defined on* $[0, T]$*, such that the following hold, for* $0 < t \le T$*:*

$$\frac{dS}{dt} = P - (\beta I_m + \epsilon_h \beta I_h)\frac{S}{N} - \mu S + \rho R, \tag{3.5}$$

$$\frac{dI_m}{dt} = (1 - \alpha^*)(\beta I_m + \epsilon_h \beta I_h)\frac{S}{N} + \gamma_h I_h - (\gamma_m + \sigma_m + \mu + d_m) I_m, \tag{3.6}$$

$$\frac{dI_h}{dt} = \alpha^*(\beta I_m + \epsilon_h \beta I_h)\frac{S}{N} + \gamma_m I_m - (\gamma_h + \sigma_h + \mu + d_h) I_h, \tag{3.7}$$

$$\frac{dR}{dt} = \sigma_m I_m + \sigma_h I_h - (\mu + \rho) R, \tag{3.8}$$

$$\frac{d\widetilde{\beta}}{dt} = \gamma_m^+ I_m + \gamma_h^+ I_h - \gamma^- \widetilde{\beta} R, \tag{3.9}$$

$$\frac{d\widetilde{\alpha^*}}{dt} = \delta_m^+ I_m + \delta_h^+ I_h - \delta^- \widetilde{\alpha^*} R, \tag{3.10}$$

where

$$\beta(t) = \Phi_\beta(\widetilde{\beta(t)}), \qquad \alpha^*(t) = \Phi_*(\widetilde{\alpha^*(t)}) \tag{3.11}$$

together with N given in (3.4). The initial conditions are

$$S(0) = S_0, \quad I_m(0) = I_{m0}, \quad I_h(0) = I_{h0}, \quad R(0) = R_{init},$$

$$\beta(0) = \beta_1, \quad \alpha^*(0) = \alpha_0^*. \tag{3.12}$$

Here, $\widetilde{\beta}$ and $\widetilde{\alpha^*}$ are the unrestricted auxiliary dependent variables, and everywhere below we refer to the restricted variables β and α^* as the infection and hospitalization rates.

We have $S_0 > 0$, the initial population before the break-out of the disease, and $I_{m0}, I_{h0} \geq 0$, $R_{init} \geq 0$, the initial populations in (3.12) at $t = 0$. Additionally, $\beta_1 \in [\beta_-, \beta_+]$ is the initial infectivity, and $\alpha_0^* \in [\alpha_-, \alpha_+]$ is the initial hospitalization rate. In practice, one typically assumes that initially $S_0 = N(0) > 0$, so that at the start, the entire population is infection-free. For the sake of generality, we assume the other initial populations are nonnegative but satisfying
$N(t) = S(t) + I_m(t) + I_h(t) + R(t)$, so that (3.4) holds at $t = 0$.

We note that (3.9) and (3.10) can be integrated as follows

$$\widetilde{\beta(t)} = \beta_1 + \int_0^t \left(\gamma_m^+ I_m(s) + \gamma_h^+ I_h(s) - \gamma^- \widetilde{\beta(s)} R(s)\right) ds,$$

$$\widetilde{\alpha^*(t)} = \alpha_0^* + \int_0^t \left(\delta_m^+ I_m(s) + \delta_h^+ I_h(s) - \delta^- \widetilde{\alpha^*(s)} R(s)\right) ds,$$

Thus (3.5)-(3.8) is a history dependent system of integral equations.

Remark 3.2.2. *We note that instead of using the restriction operators Φ_β, Φ_*, we may use the notion of the subdifferential. To that end, we let I_β, I_α be the indicator functions of $[\beta_-, \beta_+]$ and $[\alpha_-, \alpha_+]$, that is $I_\beta(\beta) = 0$ if $\beta \in [\beta_-, \beta_+]$ and $I_\beta = +\infty$*

otherwise, and similarly, $I_\alpha(\alpha^*) = 0$ *if* $\alpha \in [\alpha_-, \alpha_+]$ *and* $I_\alpha = +\infty$ *otherwise. Let* $\partial I_\beta, \partial I_\alpha$ *be the subdifferentials,*

$$\partial I_\beta(s) = \begin{cases} (-\infty, 0], & s = \beta_-, \\ 0 & \beta_- < s < \beta_+, \\ [0, \infty)) & s = \beta_+, \end{cases}$$

and similarly for ∂I_α*, with* α *replacing* β*.*

Then, instead of using restrictions, we may use the set-valued inclusions for β *and* α^**, which are*

$$\frac{d\beta}{dt} \in \Psi_\beta(I_m, I_h, R, \beta, \alpha^*) - \partial I_\beta(\beta), \quad \frac{d\alpha^*}{dt} \in \Psi_*(I_m, I_h, R, \beta, \alpha^*) - \partial I_\alpha(\alpha^*).$$

The subdifferentials guarantee that the variables cannot leave the designated intervals.

The definition of each of the parameters is provided in Table 3.1.

3.3 Analysis of the Model

In order for model 3.2.1 to be biologically feasible, it must have a solution, and all solutions that are initially nonnegative, must be non-negative and bounded. In this section we show that all three of these criteria are met.

Table 3.1: Symbols and description of parameters used in the model; the dimensional quantities are per day

Parameter	Description
P	recruitment rate of susceptible individuals
β	restricted infection transmission rate (3.11)
α^*	restricted hospitalization rate (3.11)
ϵ_h	correction factor in transmission rate by hospitalized
μ	natural death rate
d_m	disease-induced death for mildly infected
d_h	disease-induced death for hospitalized
γ_m	hospitalization rate of mildly infected
γ_h	release rate of hospitalized
σ_m	recovery rate of mildly infected
σ_h	recovery rate of hospitalized
ρ	reinfection rate of recovered
$\gamma_m^+, \gamma_h^+, \gamma^-$	infectivity change rates
$\delta_m^+, \delta_h^+, \delta^-$	hospitalization change rates
$\beta_-, \beta_+, \alpha_-, \alpha_+$	restriction intervals values
$S_0, I_{m0}, I_{h0}, R_{init},$	initial populations
β_1, α_0^*	initial rates

3.3.1 Positivity

Theorem 3.3.1. *(Positivity and estimates) Let $S_0 > 0$ and let I_{m0}, I_{h0}, R_{init} be nonnegative. If $z(t) = (S(t), I_m(t), I_h(t), R(t))$ is any solution to the system, then all of the components of z are nonnegative and uniformly bounded on each closed interval $[0, T]$ on which they exist. Then, for $0 \leq t < T$,*

$$0 \leq S, I_m, I_h, R \leq N_0 + \frac{P}{\mu}. \tag{3.13}$$

Moreover,

$$0 \leq \widetilde{\beta(t)} \leq \beta_1 + \max\{\gamma_m^+, \gamma_h^+\}(N_0 + P/\mu)T \tag{3.14}$$

and

$$0 \leq \widetilde{\alpha^*(t)} \leq \alpha_0^* + \max\{\delta_m^+, \delta_h^+\}(N_0 + P/\mu)T. \tag{3.15}$$

It follows from (3.11) that $\beta(t) \in [\beta_-, \beta_+]$ and $\alpha^*(t) \in [\alpha_-, \alpha_+]$, for $0 \leq t \leq T$.

Proof. We first assume that $I_{m0}, I_{h0,} R_{init} > 0$ and because of the continuity of the solutions, there exists a, possibly very short, time interval T^* such that $I_m(t), I_h(t), R(t) > 0$ for $0 \leq t < T^*$. Let $0 < t < T < T^*$ and denote by λ the *force of infection*

$$\lambda = \lambda(t) = \frac{\beta I_m + \varepsilon_h \beta I_h}{N}.$$

Then, $0 \leq \lambda \leq \beta(1 + \varepsilon_h)$ and (3.5) yields,

$$\frac{dS}{dt} = P - \lambda S - \mu S + \rho R \geq -(\lambda + \mu)S.$$

Using separation of variables and integration on $[0, t]$, together with the initial conditions, yields

$$S(t) \geq S_0 \exp\left(-\int_0^t \lambda(s)ds - \mu t\right) > 0,$$

since $S_0 > 0$. Similarly, for (3.6)–(3.8), we have

$$I_m(t) \geq I_{m_0} e^{-(\gamma_m+\sigma_m+d_m+\mu)t} \geq 0,$$

$$I_h(t) \geq I_{h_0} e^{-(\gamma_h+\sigma_h+d_h+\mu)t} \geq 0,$$

$$R(t) \geq R_{init} e^{-(\mu+\rho)t} \geq 0.$$

Consequently, the solution is nonnegative on $[0, T]$. The last inequality allows us to remove the restriction $T < T^*$ and also we may assume that $R_{init} \geq 0$, and so the system is nonnegative on every interval on which it exists.

Next, we show the boundedness of the solutions. By adding the first four equations of the model and using (3.4), we find

$$\frac{dN}{dt} = P - \mu N - d_m I_m - d_h I_h.$$

Hence, $\frac{dN}{dt} \leq P - \mu N$. Using separation of variables, we obtain

$$N \leq (N_0 - \frac{P}{\mu})e^{-\mu t} + \frac{P}{\mu} \leq N_0 e^{-\mu t} + \frac{P}{\mu}(1 - e^{-\mu t}) \leq N_0 + \frac{P}{\mu}.$$

Since N is bounded, and each of its components, S, I_m, I_h, and R are nonnegative, we see that all of these components are bounded as well. Next, it follows from (3.9) that

$$\widetilde{\beta}' \geq -\gamma^- \widetilde{\beta} R \geq -\gamma^- \widetilde{\beta}(N_0 + P/\mu),$$

therefore,

$$\widetilde{\beta(t)} \geq \beta_1 \exp(-\gamma^-(N_0 + P/\mu)t) > 0.$$

Also,

$$\widetilde{\beta}' \leq \gamma_m^+ I_m + \gamma_h^+ I_h \leq \max(\gamma_m^+, \gamma_h^+)(N_0 + P/\mu),$$

hence,

$$\widetilde{\beta(t)} \leq \beta_1 + \max(\gamma_m^+, \gamma_h^+)(N_0 + P/\mu)t.$$

Similarly, it follows from (3.10) that

$$\widetilde{\alpha^*(t)} \geq \alpha_0^* \exp(-\delta^-(N_0 + P/\mu)t) > 0,$$

and

$$\widetilde{\alpha^*(t)} \leq \alpha_0^* + \max(\delta_m^+, \delta_h^+)(N_0 + P/\mu)t.$$

These complete the proofs, since $0 \leq t \leq T$. □

3.3.2 Existence and Uniqueness

To establish the existence of a solution, we use the estimates above and the fact that since all the parameters are bounded, the right-hand-sides of the system are Lipschitz, and therefore the existence of the unique solution follows from standard results, see, e.g., [4]. Let $\boldsymbol{x} = \boldsymbol{x}(t) = (S, I_m, I_h, R, \widetilde{\beta}, \widetilde{\alpha^*})^T$, then the model can be written in the condensed form

$$\frac{d\boldsymbol{x}}{dt} = \mathbf{F}(\boldsymbol{x}, t), \tag{3.16}$$

where

$$\mathbf{F} = \begin{bmatrix} P - (\beta I_m + \epsilon_h \beta I_h)\frac{S}{N} - \mu S + \rho R \\ (1-\alpha^*)(\beta I_m + \epsilon_h \beta I_h)\frac{S}{N} + \gamma_h I_h - \Lambda_m I_m \\ \alpha^*(\beta I_m + \epsilon_h \beta I_h)\frac{S}{N} + \gamma_m I_m - \Lambda_h I_h \\ \sigma_m I_m + \sigma_h I_h - (\mu + \rho)R \\ \gamma_m^+ I_m + \gamma_h^+ I_h - \gamma^- \widetilde{\beta} R \\ \delta_m^+ I_m + \delta_h^+ I_h - \delta^- \widetilde{\alpha^*} R \end{bmatrix}. \tag{3.17}$$

Here, $\beta = \Phi_\beta(\widetilde{\beta})$, $\alpha^* = \Phi_*(\widetilde{\alpha^*})$, and

$$\Lambda_m = \gamma_m + \sigma_m + \mu + d_m, \qquad \Lambda_h = \gamma_h + \sigma_h + \mu + d_h.$$

It follows from the estimates in Theorem 3.3.1 that, for $0 < T < \infty$,

$$\|\boldsymbol{x}(t)\| \leq L(N_0, P, T),$$

where L is a constant that depends only on N_0, P, T and the system parameters.

As the system is Lipschitz on every arbitrary finite time interval, and globally bounded, we have global existence.

Theorem 3.3.2. *(Existence and uniqueness) Let $S_0 > 0$ and $I_{m_0}, I_{h_0}, R_{init}$, be nonnegative, $\beta_1 \in [\beta_-, \beta_+]$, $\alpha_0^* \in [\alpha_-, \alpha_+]$, and let all the coefficients be positive constants. Then, there exists a unique solution to Model 3.2.1 on every time interval $[0, T]$, for $T < \infty$.*

3.4 Stability of the DFE State

The disease-free equilibrium (DFE) is the state $S = S_0 = P/\mu$ and $I_m = I_h = R = 0$, obtained by setting the right-hand sides of the equations (3.5)-(3.8) equal to zero. We also have $\beta = \beta_1, \alpha^* = \alpha_0^*$, however, these are automatically satisfied at the $DFE = (P/\mu, 0, 0, 0)$.

We turn to finding the *basic reproduction number*, $\mathcal{R}_0$, which controls the stability of the disease-free equilibrium. We note that in what follows, the total population is kept constant, $N = S_0$.

Let $\boldsymbol{x} = (S, I_m, I_h, R, \widetilde{\beta}, \widetilde{\alpha^*})^T$, then the model can be written in a condensed form as the system (3.16) with the right-hand side given in (3.17).

To compute the Jacobian J of the system with respect to the populations, we evaluate the partial derivatives $\partial F_i/\partial x_j$ for $i, j = 1, \ldots, 4$ of $\boldsymbol{F}$ with respect to

(S, I_m, I_h, R). The matrix J is given in Section 3.7, at the end of this chapter. Here, we evaluate it at the disease free steady state $DFE = (S_0, 0, 0, 0)$. Thus,

$$J(DFE) = \begin{bmatrix} -\mu & -\beta_1 & -\epsilon_h\beta_1 & \rho \\ 0 & J_{22} & J_{23} & 0 \\ 0 & \alpha_0^*\beta_1 + \gamma_m & J_{33} & 0 \\ 0 & \sigma_m & \sigma_h & -(\mu+\rho) \end{bmatrix}. \tag{3.18}$$

where

$$J_{22} = (1-\alpha_0^*)\beta_1 - \Lambda_m, \qquad J_{23} = (1-\alpha_0^*)\epsilon_h\beta_1 + \gamma_h,$$

$$J_{33} = \alpha_0^*\epsilon_h\beta_1 - \Lambda_h.$$

The stability of the DFE is determined by the eigenvalues of $J(DFE)$. It is straightforward to see that two of the eigenvalues are

$$\lambda_1 = -\mu, \qquad \lambda_2 = -\mu - \rho. \tag{3.19}$$

Therefore, the DFE is stable and attracting if the other two eigenvalues have negative real parts. The other two eigenvalues are rather complicated, given by,

$$\lambda_{3,4} = \frac{1}{2}\left((J_{22}+J_{33}) \pm \left(4(\alpha_0^*\beta_1+\gamma_m)J_{23} + (J_{22}-J_{33})^2\right)^{1/2}\right).$$

In the simulations described in Section 3.5, we found the eigenvalues numerically. In the baseline case, we found that

$$\lambda_1 = -0.000034, \quad \lambda_2 = -0.750034, \quad \lambda_3 = -0.192912, \quad \lambda_4 = -0.968856.$$

Therefore, in the baseline case the DFE is stable and attracting.

This result is supported by the following calculation of $\mathcal{R}_0$.

3.4.1 $\underline{\mathcal{R}_0}$

We use the results in [13] to compute the "basic stability number" $\mathcal{R}_0$. To that end, consider the DFE state $(N, 0, 0, 0)$, and then $N = S = constant$, so that $P = \mu N$. We linearize the infected populations parts in $\mathbf{F}$, and following [13], we may write the reduced system as

$$\frac{dI_m}{dt} = (1 - \alpha_0^*)(\beta_1 I_m + \epsilon_h \beta_1 I_h) + \gamma_h I_h - \Lambda_m I_m, \tag{3.20}$$

$$\frac{dI_h}{dt} = \alpha_0^*(\beta_1 I_m + \epsilon_h \beta_1 I_h) + \gamma_m I_m - \Lambda_h I_h, \tag{3.21}$$

where, we recall that,

$$\Lambda_m = \gamma_m + \sigma_m + \mu + d_m, \qquad \Lambda_h = \gamma_h + \sigma_h + \mu + d_h,$$

are positive constants.

Let $\boldsymbol{x}_i = (I_m, I_h)^T$, then the linearized reduced system (3.20)–(3.21) can be written as

$$\frac{d\boldsymbol{x}_i}{dt} = \boldsymbol{G}\boldsymbol{x}_i, \tag{3.22}$$

where

$$G = \begin{bmatrix} (1 - \alpha_0^*)\beta_1 - \Lambda_m & (1 - \alpha_0^*)\epsilon_h \beta_1 + \gamma_h \\ \alpha_0^* \beta_1 + \gamma_m & \alpha_0^* \epsilon_h \beta_1 - \Lambda_h \end{bmatrix}. \tag{3.23}$$

We may write $\boldsymbol{G} = \boldsymbol{T} + \boldsymbol{\Sigma}$, where $\boldsymbol{T}$ is the *transmission* matrix and $\boldsymbol{\Sigma}$ the *transition* matrix, as

$$\boldsymbol{T} = \begin{bmatrix} (1 - \alpha_0^*)\beta_1 & (1 - \alpha_0^*)\epsilon_h \beta_1 \\ \alpha_0^* \beta_1 & \alpha_0^* \epsilon_h \beta_1 \end{bmatrix}. \tag{3.24}$$

and

$$\boldsymbol{\Sigma} = \begin{bmatrix} -\Lambda_m & \gamma_h \\ \gamma_m & -\Lambda_h \end{bmatrix}. \tag{3.25}$$

Then, the next generation matrix (NGM) $\boldsymbol{K}$ is given by

$$\boldsymbol{K} = -\boldsymbol{T}\boldsymbol{\Sigma}^{-1} = \begin{bmatrix} (1-\alpha_0^*)\beta_1 & (1-\alpha_0^*)\epsilon_h\beta_1 \\ \alpha_0^*\beta_1 & \alpha_0^*\epsilon_h\beta_1 \end{bmatrix} \times \frac{1}{\Delta} \begin{bmatrix} \Lambda_h & \gamma_h \\ \gamma_m & \Lambda_m \end{bmatrix},$$

where $\Delta = \Lambda_m\Lambda_h - \gamma_m\gamma_h$ is the determinant of $\boldsymbol{\Sigma}$. Thus,

$$\boldsymbol{K} = \frac{1}{\Delta} \begin{bmatrix} (1-\alpha_0^*)\beta_1(\Lambda_h + \epsilon_h\gamma_m) & (1-\alpha_0^*)\beta_1(\gamma_h + \epsilon_h\Lambda_m) \\ \alpha_0^*\beta_1(\Lambda_h + \epsilon_h\gamma_m) & \alpha_0^*\epsilon_h\beta_1(\gamma_h + \Lambda_m) \end{bmatrix}. \tag{3.26}$$

It is seen that $\det\boldsymbol{K} = 0$, hence the largest eigenvalue, which is $\mathcal{R}_0$, is

$$\mathcal{R}_0 = \mathrm{tr}\boldsymbol{K} = \frac{\beta_1}{\Delta}\left((1-\alpha_0^*)(\Lambda_h + \epsilon_h\gamma_m) + \alpha_0^*\epsilon_h(\gamma_h + \Lambda_m)\right). \tag{3.27}$$

In the baseline case, we found that $\mathcal{R}_0 = 0.428$, which reinforces our conclusion above that the DFE is stable and attracting, hence the disease will be eradicated, eventually.

Remark 3.4.1. *If one wishes to consider the case when asymptotically $P = P(t)$, then it is necessary to study the fibers of the global DFE attractor, see, e.g., [23]. This may be of interest in later stages of our study of such models.*

3.4.2 Endemic Equilibrium

The unusual structure of the model allows for various endemic equilibrium states (EEs), unlike the standard models. This is due to the various cases for the equilibrium values of β, α^*. We assume that an endemic equilibrium state exists and denote its populations by $\hat{S}, \hat{I}_m, \hat{I}_h, \hat{R}$, where either $\hat{I}_m > 0$, or $\hat{I}_h > 0$, or both. The

populations in such a state may depend on the signs of the terms

$$L_\beta = \gamma_m^+ \hat{I}_m + \gamma_h^+ \hat{I}_h - \gamma^- \widetilde{\beta} \hat{R}, \quad L_* = \delta_m^+ \hat{I}_m + \delta_h^+ \hat{I}_h - \delta^- \widetilde{\alpha^*} \hat{R}.$$

We assume that $\beta_s \in [\beta_-, \beta_+]$ and $\alpha_s^* \in [\alpha_-, \alpha_+]$ where $0 < \alpha_- < \alpha_+ \leq 1$, are given and fixed, within the allowed intervals. Then, at an EE, $\hat{\boldsymbol{z}} = (\hat{S}, \hat{I}_m, \hat{I}_h, \hat{R})$ is the solution of the system,

$$0 = P - \beta_s(\hat{I}_m + \epsilon_h \hat{I}_h)\frac{\hat{S}}{\hat{N}} - \mu \hat{S} + \rho \hat{R}, \tag{3.28}$$

$$0 = (1 - \alpha_s^*)\beta_s(\hat{I}_m + \epsilon_h \hat{I}_h)\frac{\hat{S}}{\hat{N}} + \gamma_h \hat{I}_h - \Lambda_m \hat{I}_m, \tag{3.29}$$

$$0 = \alpha_s^* \beta_s(\hat{I}_m + \epsilon_h \hat{I}_h)\frac{\hat{S}}{\hat{N}} + \gamma_m \hat{I}_m - \Lambda_h \hat{I}_h, \tag{3.30}$$

$$0 = \sigma_m \hat{I}_m + \sigma_h \hat{I}_h - (\mu + \rho)\hat{R}. \tag{3.31}$$

Here,

$$\hat{N} = \hat{S} + \hat{I}_m + \hat{I}_h + \hat{R}.$$

We, next, introduce the notation

$$a_1 = \frac{(1 - \alpha_s^*)\Lambda_h + \alpha_s^* \gamma_h}{\alpha_s^* \Lambda_m + (1 - \alpha_s^*)\gamma_m}, \quad a_2 = \frac{(1 - \alpha_s^*)\beta_s(a_1 + \epsilon_h)}{\Lambda_m a_1 - \gamma_h},$$

$$a_3 = \frac{\rho(\sigma_m a_1 + \sigma_h)}{\mu(\mu + \rho)} - \frac{\Lambda_m a_1 - \gamma_h}{\mu(1 - \alpha_s^*)}, \quad a_4 = \frac{\sigma_m a_1 + \sigma_h}{\mu + \rho}.$$

We conclude, based on the proof, which can be found in Section 3.7, that the solution of the endemic steady state, for the chosen β_s, α_s^* is as follows.

Proposition 3.4.2. An endemic steady state $\hat{\boldsymbol{z}} = (\hat{S}, \hat{I}_m, \hat{I}_h, \hat{R})$, corresponding to $\beta = \beta_s, \alpha^* = \alpha_s^*$, is given by

$$\hat{S} = \frac{P}{\mu} + a_3 \hat{I}_h = \frac{P}{\mu} + \frac{a_3 P(a_2 - 1)}{\mu(1 + a_1 - a_2 a_3 + a_3 + a_4)}, \tag{3.32}$$

$$\hat{I}_m = a_1 \hat{I}_h = \frac{a_1 P(a_2 - 1)}{\mu(1 + a_1 - a_2 a_3 + a_3 + a_4)}, \tag{3.33}$$

$$\hat{I}_h = \frac{P(a_2 - 1)}{\mu(1 + a_1 - a_2 a_3 + a_3 + a_4)}, \tag{3.34}$$

$$\hat{R} = \frac{\sigma_m a_1 + \sigma_h}{\mu + \rho} \hat{I}_h = \frac{(\sigma_m a_1 + \sigma_h) P(a_2 - 1)}{(\mu + \rho)\mu(1 + a_1 - a_2 a_3 + a_3 + a_4)}. \tag{3.35}$$

Moreover,

$$\hat{N} = \frac{P}{\mu} + (1 + a_1 + a_3 + a_4)\, \hat{I}_h. \tag{3.36}$$

The coefficients a_1, a_2, a_3, a_4 are given above, and the proof is given in Section 5.15.

Therefore, for each choice of $\beta_s \in [\beta_-, \beta_+]$ and $\alpha_s^* \in [\alpha_-, \alpha_+]$ there corresponds one steady state. Hence, the model has a *continuum of steady states*. This raises the question of the *reachability* of these steady states, that is, given a steady state, can we find initial conditions, different from the steady state, which guarantee that the time dependent solution converges to this state in the limit $t \to \infty$. The question is of some mathematical interest and may be studied further in the future.

It seems, and some of the simulations support the observation that when $L_\beta > 0$ then $\beta \to \beta_+$ as $t \to \infty$ and when $L_\beta < 0$ then $\beta \to \beta_-$ as $t \to \infty$. However, this is not the case for L_* and α^*. Mathematically, there are a continua of solutions, and the question of the behavior of β and α^* under specific conditions may be of interest to address in future work, as well.

3.5 Simulations

To generate the computer approximated solutions of the model, a simple explicit time-stepping algorithm was used in MATLAB. A few examples of the simulations are presented below.

The values of the various parameters for each simulation are given in Table 3.2, where the DFE column provides parameter values for the simulation depicting the system with a disease free equilibrium and the EE columns are the parameter values for the simulations depicting systems with endemic equilibria.

First, we describe the baseline simulations, the results of which are depicted in Figure 3.2. Here, the system converges to the disease-free steady state. The simulation depicts the system through $T = 50$ and illustrates the dynamics of the four populations, as well as those of β and α^*. The Susceptibles (yellow) are in the top figure, while the dynamics of the mildly infected (green), the hospitalized (maroon), and the recovered (blue), are below it. The populations converge, as $t \to \infty$, to the values $\hat{\boldsymbol{z}} = (100030, 0, 0, 0)$. The total population, eventually, consists of just the Susceptibles, since we allow Recovered to lose their immunity and become susceptible after awhile.

The dynamics of β (purple) are depicted in the third figure, and $\beta \to 0.36$ as $t \to \infty$, so it converges to the upper limit of its allowed interval. However, α^* converges to 0.0141, which is above its lower limit. This is of theoretical interest and may be worth further study. Here, $L_\beta = 0$ and $L_* = 0$.

Table 3.2: Symbols and values of the parameters in the two baseline simulations

Parameter	DFE value	EE value
P	3.4	3.4
β_1	0.2	0.18
α_0^*	0.021	0.23
ϵ_h	1.000	1.000
ρ	0.75	0.75
μ	0.000034	0.000034
d_m	0.0012	0.0005
d_h	0.0294	0.004
γ_m	0.31	0.00501
γ_h	0.1501	0.006
σ_m	0.67	0.3
σ_h	0.201	0.095
$\gamma_m^+, \gamma_h^+, \gamma^-$	$10^{-3}, 10^{-3}, 2 \times 10^{-3}$	$10^{-5}, 10^{-6}, 8 \times 10^{-5}$
$\delta_m^+, \delta_h^+, \delta^-$	$5 \times 10^{-4}, 5 \times 10^{-3}, 0.313$	$4.5 \times 10^{-4}, 7 \times 10^{-4}, 9 \times 10^{-3}$
$\beta_-, \beta_+, \alpha_-, \alpha_+$	0.1, 0.36, 0.01, 0.05	0.02, 0.25, 0.1, 0.2365
$S_0, I_{m0}, I_{h0}, R_{init},$	100,000, 20, 20, 0	7960, 787, 538, 247

Next, we consider two simulations when the system has an attracting endemic steady state (EE). The values of the parameters for both simulations are shown in Table 3.2.

The first of these simulations, Figure 3.3, shows the convergence of the solutions to the EE. Under these conditions, as $t \to \infty$, $\hat{\boldsymbol{z}} = (7763, 727, 678, 377)$, with $a_1 = 1.0729$, $a_2 = 1.2296$, $a_3 = -136.053$, $a_4 = 0.5558$. The plots in Figure 3.3

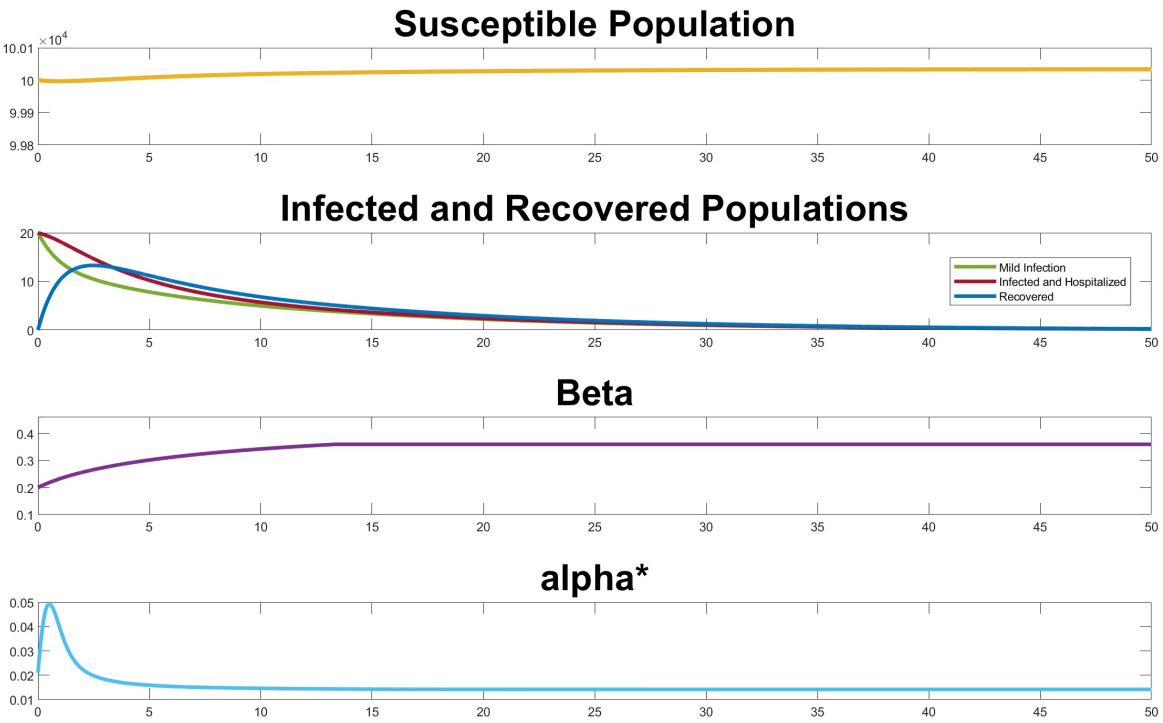

Figure 3.2: Convergence to the Disease-Free Equilibrium

depict the behavior over $0 \leq t \leq T = 500$, which visually shows the endemic behavior. When we let $T = 26,000$ (not shown), we found that each of the populations reached our calculated values for the EE under these conditions, as provided in 3.4.2. Figure 3.3 has the same form as Figure 3.2. The Susceptibles (yellow), in the top of the figure, show relatively little changes. The mildly infected (green), the hospitalized (maroon), and the recovered (blue) all show evolution initially, before reaching equilibrium. The plot of β shows that it climbs to its maximum value monotonically, whereas α^* has more variability. Though it reaches

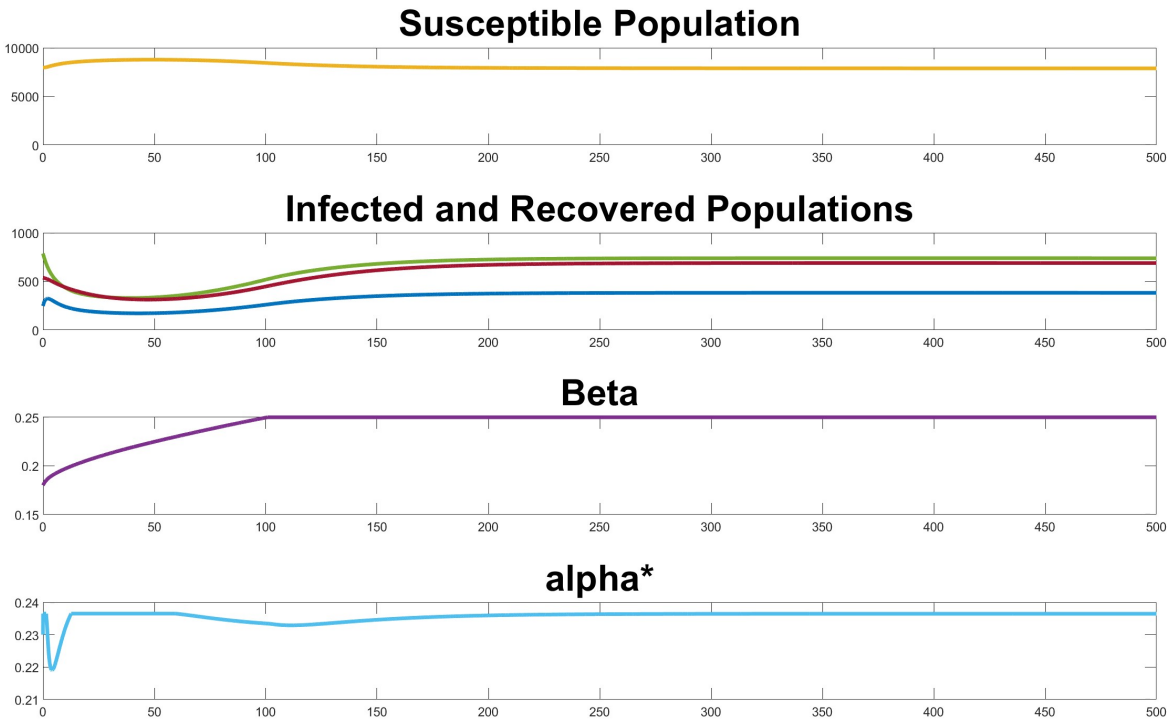

Figure 3.3: Convergence to the Endemic Equilibrium (first case)

its maximum very early, it oscillates irregularly before reaching its maximum value at equilibrium. As $t \to \infty$, $L_\beta = 0.000415$ and $L_* = 0.0891$.

The second EE simulation explores the case when at a later time ($T = 20$ in the simulation) a new variant of the pathogen appears with a higher infectivity rate in the equation for β. The values of the parameters for the second endemic simulation are the same as those in the first endemic simulation, except for the change that at $T = 20$, γ_m^+ is manually changed to 10^{-4} and γ_h^+ is changed to 10^{-5} to see how the system responds. Under these conditions, as $t \to \infty$, again we have, $\hat{\boldsymbol{z}} = (7763, 727, 678, 377)$, with $a_1 = 1.0729$, $a_2 = 1.2296$, $a_3 = -136.053$,

$a_4 = 0.5558$. We conclude that in this case the EE is attracting, and attracts the modified solutions, too.

It seems to be important to add randomness into the equations for β and α^* to include possible mutations of the pathogen and the appearance of new variants, as the case of Covid19 demonstrates. However, in light of the above example, this has to be done judiciously.

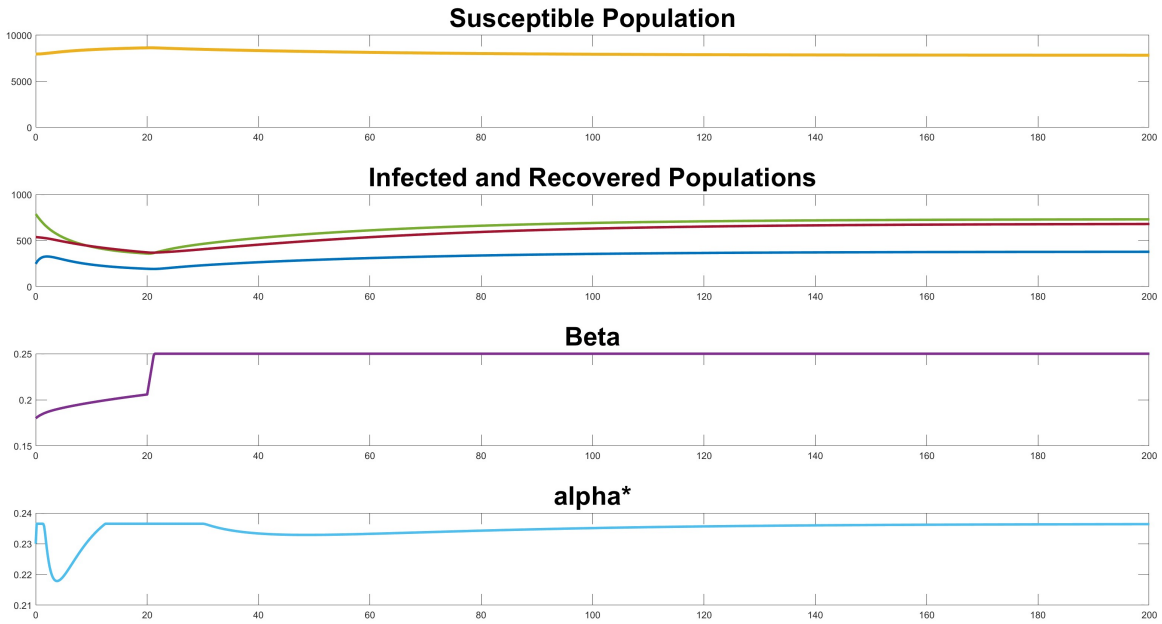

Figure 3.4: Second Endemic Equilibrium simulation. The values of the γ coefficients in (3.9) were changed at $T = 20$.

3.6 Conclusions and future work

This chapter, following [26], develops and studies, mathematically and computationally, a new extended version of the SIR model for the spread of a communicable disease in which the infected population is divided into mild or moderately sick individuals and those with a severe form who need hospitalization. The novelty lies in the assumption that the infectivity rate β and the hospitalization fraction α^*, both of which measure the severity of the disease, are system dependent variables. For simplicity, the rate equations for both variables are linear in the populations. However, it is very likely that the relationships are more complex, interesting and will need to be determined for each disease separately by some parameter identification method. We return to this point below. For the model to make epidemiological sense, both variables are limited to values in prescribed intervals, in particular, α^* is a fraction, so it is restricted to the interval $0 < \alpha_- \leq \alpha^* \leq \alpha_+ \leq 1$.

We establish the positivity and boundendess of the solutions, which lead to the proof of their existence. Then, we study the system steady states and show that in the baseline case the DFE is stable and attracting (asymptotically stable). We present two different ways to show this, the second is based on the work [13]. Then, we study cases with EE states which, because of the structure of the system, may form a continuum. These findings are supported by our computer simulations of the model. Moreover, this observation raises the question of reachability of the steady states, mentioned below.

A simple explicit time stepping algorithm was constructed and implemented, and the resulting simulations provide insight into the model predictions. The first simulation shows how the system, with stable and attracting DFE, approaches this

equilibrium. In that state only Susceptibles remain, the other populations vanish, β approaches its upper limit and α^* its lower limit.

The second simulation involves the case of an EE state that is stable and attracting. Here, the populations approach nonzero limits, as can be seen in Figure 3.3. While β converges to its upper allowed limit, the fraction of hospitalized α^* approaches a limit within its allowed interval.

The third simulation, shown in Figure 3.4, has the same parameters as the second simulation. However, to show the effect of the appearance of a more infective variant, at time $T = 20$ we changed the rate constants in the equation for β. This change leads to a jump in β. However, in the long run the solution in this case converges to the same EE limit as in the second simulation.

Some related issues and topics that warrant further study are the following:

One of the main open questions is the form of the equations for β and α^*. Assuming the form (3.1) with the restrictions (3.2), how do we find the functional forms of Ψ_β and Ψ_*? It seems to us that some statistical input is needed, as well as curve fitting to field data. The latter does not exist, yet, in a form that may be used in this model, so it needs to be developed.

The result on the existence of a continuum of steady state solutions raises the question of the *reachability* of these steady states, that is, given a steady state, can we find initial conditions which guarantee that the time dependent solution converges to this state in the limit $t \to \infty$. The topic is of interest to better understand the model.

Furthermore, it is of interest to take into account the sudden appearance of new variants of the disease agents. This may be accomplished by adding randomness to some of the system coefficients. We have begun such a study, and it seems to be of importance to continue it. It is found that simply adding random

impulses to the two equations for β and α^* does not address the issue, since the simulations show that such additions die out over time.

The addition of periodicity into some of the coefficients to take into account climate variations may be of interest.

3.7 Proof of Proposition 3.4.2

The Jacobian at the DFE: We compute the Jacobian matrix of the system. First, we note that

$$\frac{\partial(1/N)}{\partial S} = \frac{\partial(1/N)}{\partial I_m} = \frac{\partial(1/N)}{\partial I_h} = \frac{\partial(1/N)}{\partial R} = -\frac{1}{N^2}.$$

Then, the entries of J are:

$$J_{11} = \partial\mathcal{F}_1/\partial S = -(\beta I_m + \epsilon_h \beta I_h)\left(\frac{N-S}{N^2}\right) - \mu;$$

$$J_{12} = \partial\mathcal{F}_1/\partial I_m = -\beta\frac{S}{N} + (\beta I_m + \epsilon_h \beta I_h)\frac{S}{N^2};$$

$$J_{13} = \partial\mathcal{F}_1/\partial I_h = -\epsilon_h\beta\frac{S}{N} + (\beta I_m + \epsilon_h \beta I_h)\frac{S}{N^2};$$

$$J_{14} = \partial\mathcal{F}_1/\partial R = (\beta I_m + \epsilon_h \beta I_h)\frac{S}{N^2} + \rho;$$

$$J_{21} = \partial\mathcal{F}_2/\partial S = (1-\alpha^*)(\beta I_m + \epsilon_h \beta I_h)\frac{N-S}{N^2};$$

$$J_{22} = \partial\mathcal{F}_2/\partial I_m = (1-\alpha^*)\beta\frac{S}{N} - (1-\alpha^*)(\beta I_m + \epsilon_h \beta I_h)\frac{S}{N^2} - (\gamma_m + \sigma_m + \mu + d_m);$$

$$J_{23} = \partial\mathcal{F}_2/\partial I_h = (1-\alpha^*)\epsilon_h\beta\frac{S}{N} - (1-\alpha^*)(\beta I_m + \epsilon_h \beta I_h)\frac{S}{N^2} + \gamma_h;$$

$$J_{24} = \partial\mathcal{F}_2/\partial R = -(1-\alpha^*)(\beta I_m + \epsilon_h \beta I_h)\frac{S}{N^2};$$

$$J_{31} = \partial\mathcal{F}_3/\partial S = \alpha^*(\beta I_m + \epsilon_h \beta I_h)\frac{N-S}{N^2};$$

$$J_{32} = \partial\mathcal{F}_3/\partial I_m = \alpha^*\beta\frac{S}{N} - \alpha^*(\beta I_m + \epsilon_h \beta I_h)\frac{S}{N^2} + \gamma_m;$$

$$J_{33} = \partial\mathcal{F}_3/\partial I_h = \alpha^*\epsilon_h\beta\frac{S}{N} - \alpha^*(\beta I_m + \epsilon_h\beta I_h)\frac{S}{N^2} - (\gamma_h + \sigma_h + \mu + d_h);$$

$$J_{34} = \partial\mathcal{F}_3/\partial R = -\alpha^*(\beta I_m + \epsilon_h\beta I_h)\frac{S}{N^2};$$

$$J_{41} = \partial\mathcal{F}_4/\partial S = 0; \quad J_{42} = \partial\mathcal{F}_4/\partial I_m = \sigma_m; \quad J_{43} = \partial\mathcal{F}_4/\partial I_h = \sigma_h;$$

$$J_{44} = \partial\mathcal{F}_4/\partial R = -(\mu + \rho);$$

In (3.18) the entries are evaluated at the DFE.

Proof. (Proposition 3.4.2) To find solutions for the EE, we assume that $\hat{I}_m, \hat{I}_h \neq 0$, since otherwise it corresponds to the DFE. Solving for $\hat{S}/\hat{N}$ in equations (3.29) and (3.30) and setting them equal yields

$$\frac{\Lambda_m\hat{I}_m - \gamma_h\hat{I}_h}{(1-\alpha_s^*)\beta_s(\hat{I}_m + \epsilon_h\hat{I}_h)} = \frac{\Lambda_h\hat{I}_h - \gamma_m\hat{I}_m}{\alpha_s^*\beta_s(\hat{I}_m + \epsilon_h\hat{I}_h)}, \tag{3.37}$$

and consequently,

$$\hat{I}_m = a_1\hat{I}_h, \tag{3.38}$$

where

$$a_1 = \frac{(1-\alpha_s^*)\Lambda_h + \alpha_s^*\gamma_h}{\alpha_s^*\Lambda_m + (1-\alpha_s^*)\gamma_m}.$$

Solving for R in equation (3.31) and substituting the above equation for I_m gives

$$\hat{R} = \frac{\sigma_m a_1 + \sigma_h}{\mu + \rho}\hat{I}_h.$$

We now have equations for $\hat{I}_m$ and $\hat{R}$ in terms of $\hat{I}_h$, which we can substitute into equation (3.28), and we can also substitute the left-hand side of equation (3.37) in for $\hat{S}/\hat{N}$, thus,

$$\hat{S} = \frac{P}{\mu} + \left[\frac{\rho(\sigma_m a_1 + \sigma_h)}{\mu(\mu+\rho)} - \frac{\Lambda_m a_1 - \gamma_h}{\mu(1-\alpha_s^*)}\right]\hat{I}_h.$$

Since the left-hand side of equation (3.37) equals $\hat{S}/\hat{N}$, we can solve for $\hat{N}$,

$$\hat{N} = \frac{(1-\alpha_s^*)\beta_s(a_1+\epsilon_h)}{\Lambda_m a_1 - \gamma_h}\left[\frac{P}{\mu} + \left[\frac{\rho(\sigma_m a_1+\sigma_h)}{\mu(\mu+\rho)} - \frac{\Lambda_m a_1-\gamma_h}{\mu(1-\alpha_s^*)}\right]\hat{I}_h\right],$$

and, since $\hat{N}$ is also the total population, we have

$$\hat{N} = \frac{P}{\mu} + \left[\frac{\rho(\sigma_m a_1+\sigma_h)}{\mu(\mu+\rho)} - \frac{\Lambda_m a_1-\gamma_h}{\mu(1-\alpha_s^*)} + 1 + a_1 + \frac{\sigma_m a_1+\sigma_h}{\mu+\rho}\right]\hat{I}_h$$

$$= \frac{P}{\mu} + (1 + a_3 + a_1 + a_4)\,\hat{I}_h.$$

Here,

$$a_2 = \frac{(1-\alpha_s^*)\beta_s(a_1+\epsilon_h)}{\Lambda_m a_1 - \gamma_h},$$

$$a_3 = \frac{\rho(\sigma_m a_1+\sigma_h)}{\mu(\mu+\rho)} - \frac{\Lambda_m a_1-\gamma_h}{\mu(1-\alpha_s^*)},$$

$$a_4 = \frac{\sigma_m a_1+\sigma_h}{\mu+\rho}.$$

Setting the two equations for $\hat{N}$ equal gives an equation entirely in terms of $\hat{I}_h$, thus

$$a_2\left(\frac{P}{\mu} + a_3\hat{I}_h\right) = \frac{P}{\mu} + (a_3 + 1 + a_1 + a_4)\hat{I}_h.$$

And solving for $\hat{I}_h$, we obtain,

$$\hat{I}_h = \frac{P(a_2-1)}{\mu(a_3+1+a_1+a_4-a_2a_3)}.$$

□

More simulations are of interest, together with a comparison to known information about some current diseases.

As discussed in the introduction, SIR models represent a subcategory of mathematical models in epidemiology. To broaden our scope within epidemiology, we created a model to describe the effects of chemotherapy and immunotherapy on a tumor, which we present in Chapter 4.

CHAPTER FOUR

A Model for Cancer Chemo-Immunotherapy Treatment Schedules

4.1 Background

Cancer is one of the leading causes of death worldwide, and so it has garnered a lot of attention in terms of improving our understanding, treatment, and prevention of this pervasive disease. The goal of this and the subsequent chapter is to provide a tool, in the form of a mathematical model, for the scheduling of various cancer treatments alone or in combination. Such a tool and its simulations would allow for prediction of a variety of treatment scenarios that cannot be tested in the field. These chapters are the first steps in modeling the interplay of chemotherapy and immunotherapy in this chapter, which is based on [15], and chemotherapy, immunotherapy, and virotherapy in the next chapter, which is based on [14]. These models, once validated by comparison with field data, can be used to optimize combination treatment schedules.

Mathematical models are becoming more prevalent in the study of biological systems, including cancer. They are valued for their potential to provide quantitatively validated predictions, as well as their ability to provide insights into the underlying behavior of a given system. The monograph [38] describes various tools and methods, primarily from theories of dynamical systems and optimal control, for the analysis of population dynamics models for cancer and the tumor microenvironment using different treatments. An extensive survey of the optimization of mathematical models for chemotherapy treatments, in particular, can be found in [21]. This article summarizes various models applied to optimal scheduling of chemotherapy. It also classifies relevant literature on modeling

methods, providing a discussion of the limitations of existing research. Further, it provides a direction for further research in optimizing chemotherapy scheduling.

In [11, 12] mathematical models for cancer growth at the cell level and its treatments using combinations of immunotherapy and chemotherapy treatments are developed and analyzed. In these papers they study the stability of the equilibrium point and provide numerical simulations of mixed therapies using both mouse and human parameters. They indicate that combined therapies are more effective than a single therapy and combining therapies also reduces cost, time, and possible side effects, so understanding the interplay of various therapies can potentially provide myriad benefits.

Another model that is similar to the one here is [10]. It studies the conditions for local stability of all equilibrium points and the global stability condition for the tumor-free equilibrium point and provides several simulations. In [9] they present a model for iterative dynamics between effector-tumor-normal cells, which is based in part on [11]. In addition, they formulate an optimal control problem to find the best ways to administer immunotherapy to eradicate cancer without increasing the risk to patients' health. They provide numerical simulations which indicate that the optimal regimens eradicate cancer in less time than other treatments. Other models that have been constructed to study chemotherapy, immunotherapy, or a combination of the two treatments include [2, 16, 31, 34, 37, 39]

Our mathematical model, which consists of a coupled nonlinear system of ordinary differential equations (ODE's), is presented in the next section where we explain the underlying assumptions of the model and the various terms in the rate equations. The model describes the dynamics of healthy, immune, and cancer cells, as well as the dynamics of the chemotherapy and immunotherapy treatments. We allow for pulse-like administration of the chemotherapy and immunotherapy. We

then provide an analysis of the model. Solutions exist and are bounded on every finite time interval, and if the initial conditions are nonnegative, the solutions remain nonnegative. Following the analysis of the model, we analyze the steady states and the stability of the model. There we determine the basic stability number, $\mathcal{R}_0$ for the Disease-Free Equilibrium (DFE). At this point we present the results of our numerical simulations of the model using a simple time-stepping algorithm. These simulations support the conclusion that chemotherapy and immunotherapy could enhance each other and lead to better outcomes with shorter treatment schedules. We then summarize the results of our model and comment on some near-future research directions, one of which we present in Chapter 5.

4.2 The Model

The model, we have developed in [15] is a general model for the combined chemotherapy and immunotherapy of a cancer tumor. A chemotherapeutic drug and white platelets are administered to the tumor in order to eliminate it. The model allows us to study the effects of each treatment on its own, as well as the effects of various combinations of the two treatments.

The model deals with total numbers, assumes the numbers of the cells are large, so we may use continuous methods and that ODE's may be applied. We let the total number of normal or healthy cells be $H(t)$, immune cells $I(t)$, cancer tumor cells $K(t)$, and the amount of chemotherapy drug $D(t)$, all in the tumor and its immediate surroundings, at time t. Time is measured in days, and the time interval of interest is $0 \leq t \leq T$, for some $T > 0$.

The Heaviside or *cutoff function* χ_a for $a > 0$ is introduced for mathematical reasons, which we explain in detail below. It is defined as follows:

$$\chi_a(X) = \begin{cases} 0 & 0 \leq X \leq a \\ 1 & a < X. \end{cases} \tag{4.1}$$

The model we propose deals with the rates of change of the four variables as follows.

Model 4.2.1 (*Model for Chemotherapy and Immunotherapy of a Cancer Tumor*)**.** *Find four functions* $H, I, K, D : [0, T] \to \mathbb{R}^+$, *such that:*

$$\begin{aligned} \frac{dH}{dt} &= \alpha_1 H(1 - \alpha_H H) - \gamma_1 KH - \mu_1 DH - \mu_H H, & (4.2) \\ \frac{dI}{dt} &= q + \psi + \alpha_2 I(1 - \alpha_I I) - \gamma_2 KI - \mu_2 DI - \mu_I I, & (4.3) \\ \frac{dK}{dt} &= \alpha_3 K(1 - \alpha_K K)\chi_1(K) - \gamma_3 IK - \mu_3 DK - \mu_K K, & (4.4) \\ \frac{dD}{dt} &= \varphi - \beta_1 ID - \beta_2 HD - \beta_3 KD - \mu_D D. & (4.5) \end{aligned}$$

Together with the initial conditions,

$$H(0) = H_0,\ I(0) = I_0,\ K(0) = K_0,\ D(0) = D_0. \tag{4.6}$$

The rates in the model are per day, H, I, and K are all measured as populations, that is number of individual cells. The units of D are those of a drug (e.g., mg). The various terms have appropriate units (e.g., $\beta_3 KD$ and φ have units of mg drug/day, q and ψ have units of cell/day).

Equation (4.2) describes the rate of change of healthy cells per day. These cells are assumed to grow logistically with a growth rate of α_1 and a carrying capacity of $1/\alpha_H$. The healthy cell population decreases as a result of its interaction with cancer cells, which gives the term $\gamma_1 KH$. The constants μ_1 and μ_H represent the death rates due to interaction with the chemotherapy drug and the natural death rate, respectively.

Equation (4.3) describes the rate of change of immune cells. The body's natural production rate of immune cells is represented by $q = q(t)$, and the function $\psi = \psi(t)$ represents the application of immunotherapy in which white platelets are added to the tumor, thus increasing the number of immune cells. Logistic growth is assumed for these cells, as well, with the growth rate α_2 and the carrying capacity $1/\alpha_I$. The loss of immune cells due to their interaction with cancer is given by the term $\gamma_2 KI$, and similar to the healthy cells, μ_2 and μ_I represent the death rates associated with the interaction of immune cells and the chemotherapy drug and the natural death rate of immune cells, respectively.

Equation (4.4) depicts the rate of change of cancer cells. It also has a logistic term whose growth rate is α_3 and carrying capacity is $1/\alpha_K$. This logistic term requires the cutoff function χ_a because it is mathematically possible that drug administration is stopped because $K << 1$ (less than one cell), and cancer rebounds. The cutoff function forces the logistic growth term to zero when the cancer cells are below the threshold a. For the sake of simplicity, we choose $a = 1$. In reality, there may be a small number of cancer cells that survive treatment, but the body can easily take care of these without treatment. Cancer cells are also lost due to interaction with immune cells. This is represented by the term $\gamma_3 IK$. Again the two death rates are μ_3, which is due to interaction with the chemotherapy drug and μ_K, which is the natural death rate.

Equation (4.5) describes the dynamics of the chemotherapy drug. The rate at which the drug is administered is denoted $\varphi = \varphi(t)$. It is depleted by its interactions with healthy ($\beta_2 DH$), immune ($\beta_1 ID$), and cancer ($\beta_3 KD$) cells. The natural decay of the drug in vivo is $\mu_D D$.

Note that, although chemotherapy is given as a standalone equation, the immunotherapy treatment is incorporated into the equation for the dynamics of the

immune cells, since it seemed natural to consider the treatment as part of the immune system. This is why q and φ are separated, even though they are both inflowing immune cells. The immunotherapy treatment is visible in the system as φ.

To complete the model, we prescribe the initial cell populations and the initial drug amount. To adhere to biological principles, we assume

$$H(0) = H_0 \in (0, 1/\alpha_H),\ I(0) = I_0 \in (0, 1/\alpha_I),\ K(0) = K_0 \in (1, 1/\alpha_K),$$

$$D(0) = D_0 > 0. \tag{4.7}$$

4.3 Analysis of the Model: Existence, Positive Invariance, and Boundedness

In this section, we show that the solutions to the model exist, are positively invariant, and are bounded. Since the right-hand sides are locally Lipschitz continuous, the system (4.2) - (4.5) has a local solution. The initial conditions (4.6) guarantee that there exists $0 < t_0$ such that the solution exists on the time interval $[0, t_0]$, where it is nonnegative and bounded. Let C^* denote the bound of all the variables on $[0, t_0]$. If we can show that the model is biologically feasible, in other words, nonnegative initial conditions imply that all solutions will remain nonnegative and we have that the solutions are bounded on arbitrary finite time intervals, we establish global solvability on every time interval.

Proposition 4.3.1. Assume that the initial conditions satisfy (4.7) and q, φ and ψ are Lipschitz, nonnegative and bounded functions, say $0 \leq q, \varphi, \psi \leq M$. And let

$$\Delta = \sqrt{\alpha_2^2 + 8\alpha_2\alpha_I M},$$

Then, every solution of system (4.2)–(4.5) satisfies the estimates:

$$0 < H \leq \frac{H_0}{(1 - \alpha_H H_0)e^{-\alpha_1 T} + H_0\alpha_H} \leq \frac{1}{\alpha_H}, \tag{4.8}$$

$$0 < I \leq \frac{\alpha_2 + \Delta}{2\alpha_2\alpha_I}, \tag{4.9}$$

$$0 \leq K \leq \frac{K_0 e^{\alpha_3 T}}{1 - \alpha_K K_0 + K_0\alpha_K e^{\alpha_3 T}} \leq \frac{1}{\alpha_K}, \tag{4.10}$$

$$0 \leq D \leq D_0 + \frac{2M}{\mu_D}, \tag{4.11}$$

on every interval $[0, T]$, for $0 < T < \infty$.

We conclude that the **feasible region** Ω is

$$\Omega = \left\{ (H, I, K, D) \in R_+^4 : \ H(t) \in \left(0, \frac{1}{\alpha_H}\right], \quad I(t) \in \left(0, \frac{\alpha_2 + \Delta}{2\alpha_2\alpha_I}\right], \right.$$
$$\left. K(t) \in \left[0, \frac{1}{\alpha_K}\right], \quad D(t) \in \left[0, D_0 + \frac{2M}{\mu_D}\right] \right\}$$

which is positively invariant for the system (4.2)-(4.5).

Proof. The initial conditions are assumed to be positive. By the continuity of the solutions, there must exist some time interval $[0, t_0]$, $t_0 > 0$ on which the solutions remain nonnegative and bounded by some positive constant C^*.

From equation (4.2) and the nonnegative constants and initial conditions, it must be true that

$$\frac{dH}{dt} \leq \alpha_1 H(1 - \alpha_H H).$$

Let $\tilde{H}$ be the solution of the logistic equation

$$\frac{d\tilde{H}}{dt} = \alpha_1 \tilde{H}(1 - \alpha_H \tilde{H}), \quad \tilde{H}(0) = H_0,$$

then $H \leq \tilde{H}$. By using partial fraction decomposition, we can arrive at

$$\left(\frac{1}{\tilde{H}} + \frac{\alpha_H}{1 - \alpha_H \tilde{H}}\right) d\tilde{H} = \alpha_1 dt,$$

which implies that

$$H \leq \tilde{H} = \frac{H_0}{(1 - \alpha_H H_0)e^{-\alpha_1 T} + H_0 \alpha_H} \leq \frac{1}{\alpha_H}.$$

To get the lower bound, we use the fact that

$$\frac{dH}{dt} \geq -(\alpha_1 \alpha_H C^* + \gamma_1 C^* + \mu C^* + \mu_H)H \geq -c_1 H,$$

where $c_1 > 0$. Thus, we have

$$H(t) \geq H_0 e^{-c_1 t} > 0.$$

which is estimate (4.8). Estimate (4.10) is derived similarly. The cutoff function χ in (4.4) does not change the estimates. It actually makes it slightly easier to calculate.

To obtain estimate (4.9), we follow the same approach using (4.3).

$$\frac{dI}{dt} \leq q + \psi + \alpha_2 I(1 - \alpha_I I) \leq 2M + \alpha_2 I(1 - \alpha_I I),$$

and so we have

$$\frac{dI}{2M + \alpha_2 I(1 - \alpha_I I)} \leq dt.$$

Here, we use separation of variables, let

$$\Delta = \sqrt{\alpha_2^2 + 8\alpha_2 \alpha_I M},$$

and factor the numerator to obtain

$$\frac{-dI}{\alpha_2\alpha_I\left(I-\frac{\alpha_2+\Delta}{2\alpha_2\alpha_I}\right)\left(I-\frac{\alpha_2-\Delta}{2\alpha_2\alpha_I}\right)} \leq dt.$$

Partial fraction decomposition yields

$$\frac{1}{\Delta}\left[\frac{-1}{\left(I-\frac{\alpha_2+\Delta}{2\alpha_2\alpha_I}\right)}+\frac{1}{\left(I-\frac{\alpha_2-\Delta}{2\alpha_2\alpha_I}\right)}\right]dI \leq dt.$$

Integrating gives

$$\frac{1}{\Delta}\log\left|\frac{\alpha_2(1-2\alpha_I I)-\Delta}{\alpha_2(1-2\alpha_I I)+\Delta}\right| \leq t+C,$$

where C is an integration constant, determined by the initial condition $I(0)=I_0$.

$$\frac{1}{\Delta}\log\left|\frac{\alpha_2(1-2\alpha_I I)-\Delta}{\alpha_2(1-2\alpha_I I)+\Delta}\right| \leq t+\frac{1}{\Delta}\log\left|\frac{\alpha_2(1-2\alpha_I I_0)-\Delta}{\alpha_2(1-2\alpha_I I_0)+\Delta}\right|,$$

which yields

$$\left|\frac{\alpha_2(1-2\alpha_I I)-\Delta}{\alpha_2(1-2\alpha_I I)+\Delta}\right| \leq \left|\frac{\alpha_2(1-2\alpha_I I_0)-\Delta}{\alpha_2(1-2\alpha_I I_0)+\Delta}\right| e^{\Delta t}.$$

For this inequality to be true, it must be that

$$-\left|\frac{\alpha_2(1-2\alpha_I I_0)-\Delta}{\alpha_2(1-2\alpha_I I_0)+\Delta}\right| e^{\Delta t} \leq \frac{\alpha_2(1-2\alpha_I I)-\Delta}{\alpha_2(1-2\alpha_I I)+\Delta}.$$

Letting

$$Q=\frac{\alpha_2(1-2\alpha_I I_0)-\Delta}{\alpha_2(1-2\alpha_I I_0)+\Delta}$$

and noting that Δ is positive and large so that $Q<0$, we can solve for I.

$$I \leq \frac{(\alpha_2+\Delta)Q+(\alpha_2-\Delta)e^{-\Delta t}}{2\alpha_2\alpha_I Q+(2\alpha_2\alpha_I)e^{-\Delta t}} \leq \frac{\alpha_2+\Delta}{2\alpha_2\alpha_I},$$

We also have

$$\frac{dI}{dt} \geq -(\alpha_2\alpha_I+\gamma_2 K+\mu_2 D+\mu_I)I \geq -c_2 I,$$

which indicates

$$I \geq I_0 e^{-c_2 t} > 0.$$

Equation (4.5) satisfies,

$$\frac{dD}{dt} \leq \varphi - \mu_D D \leq M - \mu_D D,$$

which leads to

$$D \leq \frac{M}{\mu_D} + \left| D_0 - \frac{M}{\mu_D} \right| e^{-\mu_D t} \leq D_0 + \frac{2M}{\mu_D},$$

and

$$\frac{dD}{dt} \geq -(\beta_1 I + \beta_2 H + \beta_3 K + \mu_D) D,$$

therefore,

$$D \geq D_0 e^{-c_3 t} \geq 0.$$

□

This result shows that the system is Lipschitz on every arbitrary finite time interval. We have the following global existence result.

Theorem 4.3.2 (Global Existence, part 1)**.** *Assume that the initial conditions satisfy (4.7) and q, φ, and ψ are smooth, positive and bounded functions. Then, system (4.2)–(4.5) has a unique smooth solution on every time interval* $[0, T]$, $0 < T \leq \infty$.

4.4 Stability

Equilibria are found by equating the derivatives to zero. However, in our case, the equilibrium points are only of mathematical interest, since the purpose of

the model is to find ways to drive the system as quickly as possible to the DFE, the state without cancer.

Let $(\bar{H}, \bar{I}, \bar{K}, \bar{D})$ denote the equilibrium values. The equilibrium system (omitting the bars) is as follows:

$$\begin{aligned} \alpha_1 H(1-\alpha_H H) - \gamma_1 KH - \mu_1 DH - \mu_H H = 0, \\ q + \psi + \alpha_2 I(1-\alpha_I I) - \gamma_2 IK - \mu_2 DI - \mu_I I = 0, \\ \alpha_3 K(1-\alpha_K K)\chi_1(K) - \gamma_3 IK - \mu_3 DK - \mu_K K = 0, \\ \varphi - \beta_1 DI - \beta_2 DH - \beta_3 DK - \mu_D D = 0. \end{aligned} \tag{4.12}$$

For biological reasons, we assume everywhere below that the growth rate constants are larger than the death rate constants,

$$\alpha_1 > \mu_H, \qquad \alpha_2 > \mu_I, \qquad \alpha_3 > \mu_K. \tag{4.13}$$

4.4.1 Disease-Free Equilibrium

To study the DFEs, we observe that we need K, D, ψ,and φ to equal 0, since neither the drug nor the immunotherapy are needed. Moreover, q is a positive constant. Thus, we have a reduced system,

$$\alpha_1 H(1-\alpha_H H) - \mu_H H = 0,$$

$$q + \alpha_2 I(1-\alpha_I I) - \mu_I I = 0.$$

The first equation has two solutions, $H_1 = \dfrac{\alpha_1 - \mu_H}{\alpha_1 \alpha_H}, H_2 = 0$. The second equation also has two solutions:

$$I_{1,2} = \frac{(\alpha_2 - \mu_I) \pm \sqrt{(\alpha_2 - \mu_I)^2 + 4\alpha_2 \alpha_I q}}{2\alpha_2 \alpha_I}.$$

We note that the solution I_1 is positive, since $\alpha_2 > \mu_I$, while I_2 is negative, which we disregard as a mathematical artifact, since Proposition 4.3.1 states the solutions are nonnegative for all t. Therefore, we find four DFE solutions (H, I, K, D). However, the two solutions with $H_2 = 0$ are of no interest and neither is I_2. Therefore, we consider the only feasible solution $(H_1, I_1, 0, 0)$. The stability of the DFE is studied below.

We use the values for the numerical simulations, presented in Section 4.5, to explore the case of convergence to a DFE. It was found that

$$(H, I, K, D) = (995, 1127, 0, 0). \tag{4.14}$$

To obtain the stability of the DFE, we computed the Jacobian of the system, given by

$$J(H, I, K, D) = \begin{bmatrix} J_{11} & 0 & -\gamma_1 H & -\mu_1 H \\ 0 & J_{22} & -\gamma_2 I & -\mu_2 I \\ -\gamma_4 K & -\gamma_3 K & J_{33} & -\mu_3 K \\ -\beta_2 D & -\beta_1 D & -\beta_3 D & J_{44} \end{bmatrix}, \tag{4.15}$$

Where the terms J_{11}, J_{22}, J_{33}, and J_{44} are:

$$J_{11} = \alpha_1(1 - 2\alpha_H H) - \gamma_1 K - \mu_1 D - \mu_H,$$

$$J_{22} = \alpha_2(1 - 2\alpha_I I) - \gamma_2 K - \mu_2 D - \mu_I,$$

$$J_{33} = \alpha_3(1 - 2\alpha_K K) - \gamma_3 I - \mu_3 D - \mu_K,$$

$$J_{44} = -\beta_1 I - \beta_2 H - \beta_3 K - \mu_D.$$

Then in the DFE, we have

$$J_{11} = (\alpha_1 - \mu_H) - 2\alpha_1\alpha_H = -(\alpha_1 - \mu_H) < 0,$$

$$J_{22} = (\alpha_2 - \mu_I) - 2\alpha_2\alpha_I = -\hat{\Delta} < 0,$$

$$J_{33} = (\alpha_3 - \mu_K) - \gamma_3 I = (\alpha_3 - \mu_K) - \gamma_3 \frac{(\alpha_2 - \mu_I) + \hat{\Delta}}{2\alpha_2\alpha_I}.$$

$$J_{44} = -\beta_1 I - \beta_2 H - \mu_D = -\beta_2 \frac{\alpha_1 - \mu_H}{\alpha_1\alpha_H} - \mu_D - \beta_1 \frac{(\alpha_2 - \mu_I) + \hat{\Delta}}{2\alpha_2\alpha_I} < 0,$$

where

$$\hat{\Delta} = \sqrt{(\alpha_2 - \mu_I)^2 + 4\alpha_2\alpha_I q}.$$

Hence,

$$J(H, I, 0, 0) = \begin{bmatrix} J_{11} & 0 & -\gamma_1 H & -\mu_1 H \\ 0 & J_{22} & -\gamma_2 I & -\mu_2 I \\ 0 & 0 & J_{33} & 0 \\ 0 & 0 & 0 & J_{44} \end{bmatrix}.$$

Since $J_{11} < 0$, $J_{22} < 0$, and $J_{44} < 0$, the stability of the DFE depends on the sign of J_{33}. We conclude

Proposition 4.4.1. Assume that (4.13) holds. The DFE is stable and attracting when

$$(\alpha_3 - \mu_K) < \gamma_3 \frac{(\alpha_2 - \mu_I) + \hat{\Delta}}{2\alpha_2\alpha_I}.$$

The DFE is only stable when equality holds. The DFE is unstable when the inequality is reversed.

We conclude that the basic stability number is

$$\mathcal{R}_0 = \frac{2\alpha_2\alpha_I(\alpha_3 - \mu_K)}{\gamma_3\left(\alpha_2 - \mu_I + \hat{\Delta}\right)}. \tag{4.16}$$

Using the baseline simulations, we find that $\mathcal{R}_0 = 0.0295$, thus the DFE is stable and attracting.

4.4.2 Endemic Equilibrium

Our main interest in this work is in eradication of the cancer cells, hence the endemic equilibrium is of no interest here. For the sake of completeness, we just provide the following brief description.

To find the endemic equilibria (EE) we assume that q and φ are positive constants, since it is necessary to use the chemo to keep the cancer at a steady nonzero level, but $\psi = 0$. The system now is the full system, indeed,

$$\alpha_1 H(1 - \alpha_H H) - \gamma_1 KH - \mu_1 DH - \mu_H H = 0,$$

$$q + \psi + \alpha_2 I(1 - \alpha_I I) - \gamma_2 IK - \mu_2 DI - \mu_I I = 0,$$

$$\alpha_3 K(1 - \alpha_K K) - \gamma_3 IK - \mu_3 DK - \mu_K K = 0,$$

$$\varphi - \beta_1 DI - \beta_2 DH - \beta_3 DK - \mu_D D = 0.$$

Simple manipulations, using the fact that $H > 0$ and $K > 1$, otherwise $K = 0$, hence $\chi_1(K) = 1$, yield

$$\alpha_1\alpha_H H + \gamma_1 K + \mu_1 D = \alpha_1 - \mu_H,$$

$$q + \psi + \alpha_2 I(1 - \alpha_I I) - \gamma_2 IK - \mu_2 DI - \mu_I I = 0,$$

$$\alpha_3\alpha_K K + \gamma_3 I + \mu_3 D = \alpha_3 - \mu_K,$$

$$\varphi - \beta_1 DI - \beta_2 DH - \beta_3 DK - \mu_D D = 0.$$

Therefore,

$$H = \frac{1}{\alpha_1\alpha_H}\left(\alpha_1 - \mu_H - \gamma_1 K - \mu_1 D\right);$$

$$I = \frac{1}{\alpha_2\alpha_I}\left((\alpha_2 - \gamma_2 K - \mu_2 D - \mu_I) + \sqrt{(\alpha_2 - \gamma_2 K - \mu_2 D - \mu_I)^2 + 4\alpha_2\alpha_I(q + \psi)}\right);$$

$$K = \frac{1}{\alpha_3 \alpha_K} \left(\alpha_3 - \mu_K - \gamma_3 I - \mu_3 D \right);$$

and finally, the amount of chemo needed to maintain EE is

$$D = \frac{\varphi}{\beta_1 I + \beta_2 H + \beta_3 K + \mu_D}.$$

Clearly, the system is highly nonlinear and is not easy to solve explicitly. Indeed, using symbolic algebra leads to very convoluted expressions.

4.5 Simulations

To obtain insight into the model's solutions, that is, to compute approximate solutions of the model, we constructed an explicit time-stepping algorithm and wrote the program in MATLAB. The purpose of the simulations is to show a typical behavior of the model, and then to compare the results when only chemotherapy is administered, only immunotherapy is used, and when both are applied.

We discretized the time interval T into N subintervals of length $\Delta t = T/N$. Typically, in the simulations, we use $\Delta t = 4.5872$ x 10^{-4}. Denoting the value of a function f at time $t_n = n\Delta t$ by f^n, we consider the discretized system, for $n = 0, 1, \ldots N-1$,

$$H^{n+1} = H^n + (\alpha_1 H^n (1 - \alpha_H H^n) - \gamma_1 K^n H^n - \mu_1 D^n H^n - \mu_H H^n)\, \Delta t, \tag{4.17}$$

$$I^{n+1} = I^n + (q^n + \psi^n + \alpha_2 I^n (1 - \alpha_I I^n) - \gamma_2 K^n I^n - \mu_2 D^n I^n - \mu_I I^n)\, \Delta t, \tag{4.18}$$

$$K^{n+1} = K^n + (\alpha_3 K^n (1 - \alpha_K K^n) \chi_1(K^n) - \gamma_3 I^n K^n - \mu_3 D^n K^n - \mu_K K^n)\, \Delta t, \tag{4.19}$$

$$D^{n+1} = D^n + (\varphi^n - \beta_1 I^n D^n - \beta_2 H^n D^n - \beta_3 K^n D^n - \mu_D D^n)\, \Delta t, \tag{4.20}$$

together with the initial conditions,

$$H^0 = H_0,\ I^0 = I_0,\ K^0 = K_0,\ D^0 = D_0. \tag{4.21}$$

As shown in the above discretization of the model equations, we applied Euler's Method to generate approximate solutions to our system.

Since the model is new and generic, we experimented with the values of the various parameters, using 'reasonable' values, to obtain the different possible types of behavior of the system. Since our main interest is to eradicate the disease, we do not dwell on the EE equilibrium, nor on the various other types of behavior generated by the code.

4.5.1 Baseline - DFE

First, we describe the baseline simulations that correspond to a DFE. Table 4.1 provides the system coefficients in this case. Using these parameter values together with the initial values $H_0 = 500$, $I_0 = 525$, $K_0 = 600$, and $D_0 = 0$, we obtain the results depicted in Figure 4.1. To obtain the DFE we truncate the chemo source function φ and set it to zero at times $t \geq 30$. The chemotherapy provided up until this time is sufficient to kill the tumor in the simulation, so chemotherapy beyond $t = 30$ is not needed. Healthy and immune cells initially decrease, stabilize and then increase monotonically to their steady state values, predicted in (4.14), which are

$$\bar{H} = 995, \qquad \bar{I} = 1127.$$

The cancer cells, and therefore the disease, vanish after 50 days. Here, we used the cutoff function χ_1 and set $K = 0$ when the value of K dropped below 1.

Table 4.1: Symbols and the values of the baseline parameters

Parameter	Value	Description
q	40	rate of supply of immune cells
φ	170	rate at which drug is administered (variable)
α_1	0.1	maximal growth rate constant of healthy cells
α_2	0.2	maximal growth rate constant of immune cells
α_I	0.001	reciprocal of immune cell carrying capacity
α_H	0.001	reciprocal of healthy cell carrying capacity
α_3	0.5	maximal growth rate constant of tumor cells
α_K	0.001	reciprocal of tumor cell carrying capacity
γ_1	0.001	loss rate of healthy cells due to tumor cells
γ_2	0.015	loss rate of immune cells due to tumor cells
γ_3	0.015	loss rate of cancer cells due to immune cells
μ_1	0.001	death rate of healthy cells due to drug
μ_H	0.0005	natural mortality rate of healthy cells
μ_2	0.001	rate at which drug kills immune cells
μ_I	0.01	natural death rate of immune cells
μ_3	0.05	death rate of cancer cells due to drug
μ_K	0.001	natural death rate of cancer cells
μ_D	0.1	natural decay in vivo of the drug
β_1	0.01	drug decrease due to immune cells
β_2	0.5	drug decrease due to cancer cells
β_3	0.01	drug decrease due to normal cells

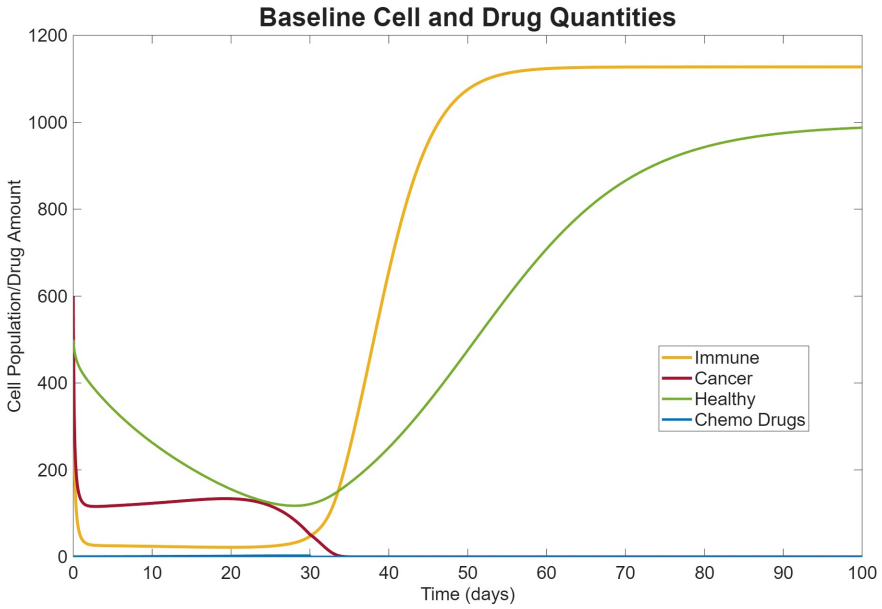

Figure 4.1: The baseline DFE with data in Table 4.1. The chemo was discontinued ($\varphi = 0$) after 30 days. Cancer vanishes ($K < 1$ hence $K = 0$) at day $t = 32$. The vertical axis is population/drug amount, the horizontal axis is time in days.

We conclude that the model predicts the healing from the disease under these conditions. Substituting the parameter values in the expression (4.16) yields $\mathcal{R}_0 = 0.0295$, which shows that the DFE is, indeed, stable and attracting (asymptotically stable).

For completeness, Figure 4.2 shows the behavior of the system using the same parameters, but without the chemo drug. It is clear that cancer cells grow to their steady state, at the expense of healthy and immune cells. Thus, without the chemo drug, the DFE is unstable.

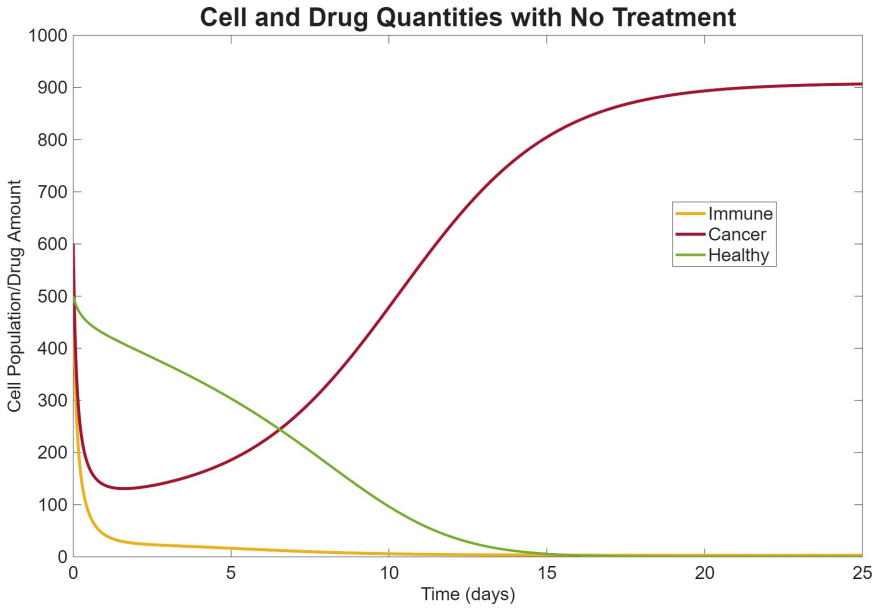

Figure 4.2: The baseline case, Table 4.1, but without the chemo drug ($D = 0$). At $t = 25$ cancer reaches close to its carrying capacity and stays there, while the other cell populations collapse.

4.5.2 Weekly chemotherapy or immunotherapy

We turn to the main interest of this chapter, namely, the simulations of weekly cancer treatments. The choice of weekly administration of the chemotherapy drug and immunotherapy was based on information we received from cancer specialists. However, it is only one regimen of many possible time schedules found in the literature.

The first case is when only chemotherapy is administered weekly, and the second case is when only immunotherapy is administered weekly. The parameters used in these two simulations are given in Table 4.2. The only difference between the two cases is that in the first case $\psi = 0$ and in the second case $\varphi = 0$.

Table 4.2: Symbols and values of the parameters in the simulations of weekly administering of chemotherapy and weekly administering of immunotherapy

Parameter	Weekly chemo	Weekly immunotherapy
q	40	40
ψ	0	707
φ	3200	0
α_1	0.1	0.1
α_2	0.2	0.2
α_I	0.001	0.001
α_H	0.001	0.001
α_3	0.5	0.5
α_K	0.001	0.001
γ_1	0.001	0.001
γ_2	0.0146	0.0146
γ_3	0.015	0.015
μ_1	0.001	0.001
μ_H	0.0005	0.0005
μ_2	0.001	0.001
μ_I	0.01	0.01
μ_3	0.25	0.25
μ_K	0.001	0.001
μ_D	0.1	0.1
β_1	0.01	0.01
β_2	0.5	0.5
β_3	0.01	0.01

In the first case, we use a chemo drug that is administered on day 8, and once every week afterwards, for four rounds of treatment,

$$\varphi = \begin{cases} 3200 & t = 8, 15, 22, 29, \\ 0 & \text{otherwise.} \end{cases}$$

As was noted in Section 4.2, the units of φ are drug quantity/day.

For mathematical reasons, we may consider an appropriate Lipschitz continuous approximation of φ, to avoid delta-like inputs.

The simulation results are shown in Figure 4.3. Immediately after each of the applications the number of cancer cells sharply decreases and then until the fourth application. There is a considerable decrease in the number of healthy and immune cells because of their interaction with cancer cells. However, on day 28, after the fourth installment of the chemo treatment, cancer decreases dramatically and then dies around day $t = 32$. Once cancer disappears, immune and healthy cell populations rebound and monotonically approach their steady-state levels of $\bar{H} = 995$ and $\bar{I} = 1127$.

We turn to the case of weekly treatment with immunotherapy. We note that while the dynamics of the chemo drug are represented by equation (4.5), where treatment is represented by φ, the administration of immunotherapy ψ is included in the dynamics of the immune cell population.

We follow a similar pattern as above and assume that the immunotherapy is administered once a week, starting on day $t = 8$, for four consecutive weeks, until day $t = 29$,

$$\psi = \begin{cases} 707 & t = 8, 15, 22, 29; \\ 0 & \text{otherwise.} \end{cases}$$

As was noted in Section 4.2, the units are cells/day.

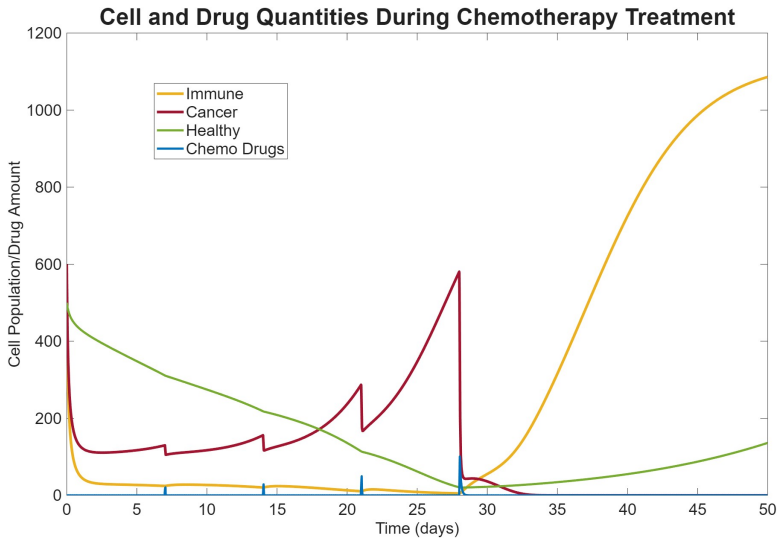

Figure 4.3: Weekly administered chemo drug (blue). Cancer (red) vanished ($K < 1$) after the fourth dose; then the healthy and immune cell populations increase monotonically towards their steady states.

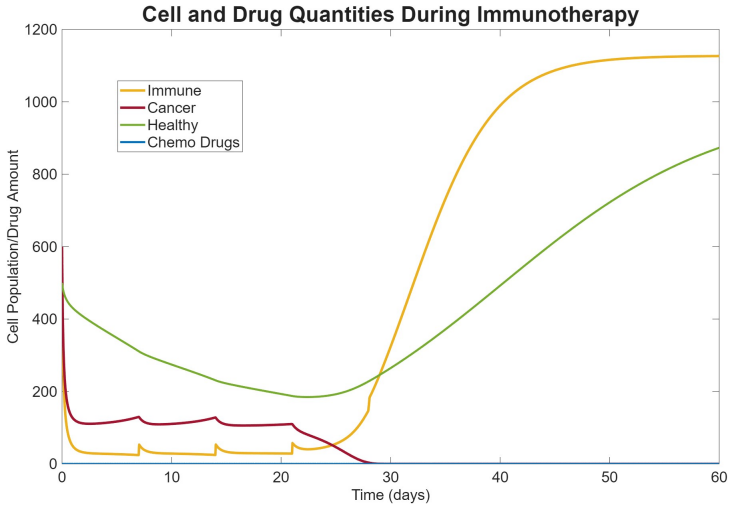

Figure 4.4: Weekly administered immunotherapy; without the chemo drug, $D = 0$. Cancer vanishes ($K < 1$) after the third dose, and then the other populations increase toward their steady states.

The simulation results are shown in Figure 4.4. The number of cancer cells decreases after each immunotherapy dose, but then it grows following the first two applications. The number vanishes after the third application. A decrease in the number of healthy and immune cells is evident as a result of their interaction with cancer cells. Once cancer disappears, immune and healthy cell populations recover and approach monotonically their steady-state levels of $\bar{H} = 995$ and $\bar{I} = 1127$.

4.5.3 Combined chemotherapy and immunotherapy

We now describe three computer experiments of the effects of the combined treatments. The first experiment, depicted in Figure 4.5, represents a weekly administration of alternating chemotherapy and immunotherapy, beginning with chemotherapy, using the same source functions φ and ψ as above. Cancer vanishes after the three doses of chemotherapy and two immunotherapy treatments and then,

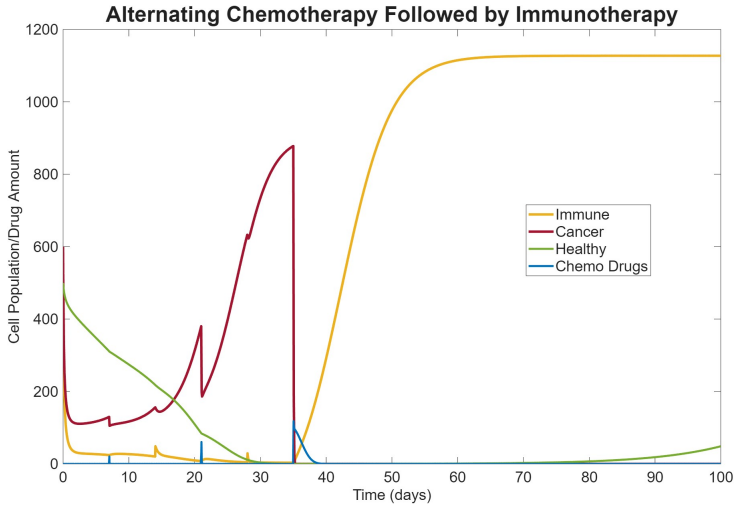

Figure 4.5: Weekly administered chemotherapy and immunotherapy alternately, beginning with chemotherapy. Cancer vanished after three doses of chemotherapy and two immunotherapy treatments; then the other populations increase toward their steady states.

as above, the other populations recover and grow towards their steady states. However, it is seen that the level of the cancer cells reaches much higher peaks, before disappearing after the fifth treatment (the third chemotherapy).

Figure 4.6 shows the experiment when immunotherapy is administered first and then chemotherapy. It is found that cancer disappears after the third treatment (the second immunotherapy). The cancer dynamics here are similar to the simulation with only immunotherapy, in that only three treatments are required, and the cancer disappears around the 28th day.

Finally, Figure 4.7 shows the case when both chemotherapy and immunotherapy are administered on the same day. It is very interesting to note that a single application of both therapies at the same time is enough to kill the cancer population. This is a very interesting prediction of the model; however, it needs field verification.

4.6 Conclusions and future work

Our results indicate that combined therapies are more effective than a single therapy given alone. These results must be taken with caution, as the model is not yet validated, which is our next objective. However, once it is validated, it has the potential to indicate more effective cancer treatment schedules, improving patient care, cost, time, and overall use of medical facilities. In addition to validating the model, we are also considering performing a parameter sensitivity analysis, adding randomness to the system to make it more realistic, and studying the attractors in the system to find if the model supports chaos. Another consideration for future work was to add other possible treatments. Since virotherapy is an emerging treatment of cancer, we decided to include it in a follow-up model. In Chapter 5 we

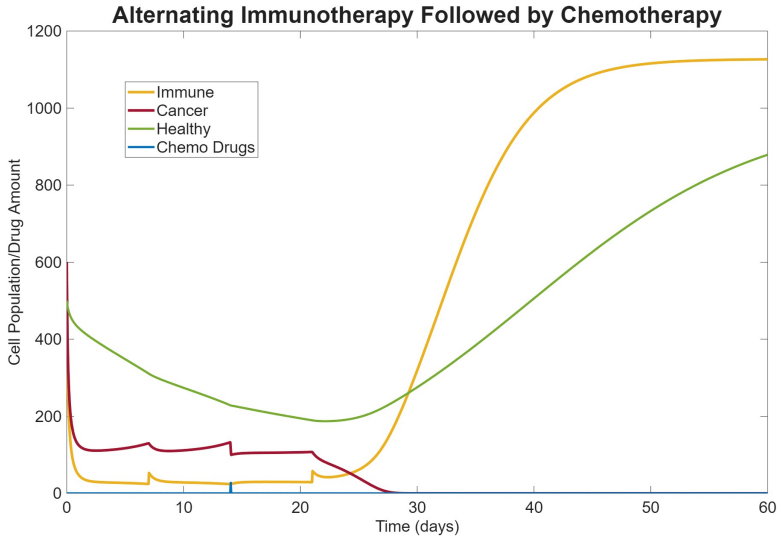

Figure 4.6: Weekly administered alternating chemotherapy and immunotherapy, beginning with immunotherapy. Cancer vanished after two immunotherapy and one chemotherapy treatments, then the other populations increase toward their steady states.

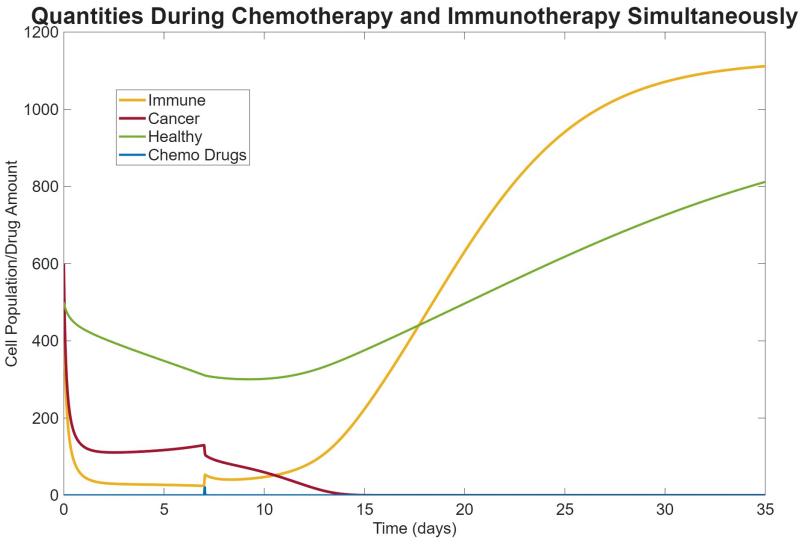

Figure 4.7: Weekly administered both chemotherapy and immunotherapy together. Cancer vanished after first dose, other populations increase toward their steady states.

present this model, which considers the effects of chemotherapy, immunotherapy, and virotherapy on a tumor.

CHAPTER FIVE

A Mathematical Model for Chemotherapy, Immunotherapy and Virotherapy Treatments of Cancer

5.1 Background

Oncolytic virotherapy is an emerging and promising cancer treatment that uses genetically modified or naturally occurring viruses to selectively target and kill cancer cells. This chapter, which is based on [14], builds on the previous one by considering a treatment plan that potentially includes chemotherapy, immunotherapy, and virotherapy. The strategy behind virotherapy is to make use of the fact that certain viruses are able to selectively infect and multiply inside living cells. In oncolytic virotherapy, viruses are modified to target certain traits specific of tumors, thereby inflicting less harm on nearby healthy cells than some other treatments. Virotherapy can also mitigate some of the negative effects of traditional therapies, including non-specific toxicity and drug resistance. Oncolytic virotherapy is one of three main branches of anticancer virotherapy. The other two are viral vector-based vaccines and viral vector-based gene therapy. Three main groups of viruses are dsDNA viruses (e.g. Adenoviruses, Herpesviruses, and Poxviruses), ssDNA viruses (+ strand or "sense") DNA (e.g. Parvoviruses), and dsRNA viruses (e.g. Reoviruses), [41]. Our interest is in the dsDNA viruses.

Pooladvand [35] created a mathematical model using a system of partial differential equations to examine how viral infectivity affects the interactions between oncolytic viruses and tumor cells. The model describes the spatial and temporal dynamics of uninfected tumor cells, infected tumor cells, and free viral particles within a spherically symmetric tumor environment. The infectivity parameter, which measures the virus's capacity to be internalized by tumor cells

that are not infected, is a key aspect of the model. This parameter, which is derived from experimental data, takes into account the changes in the tumor microenvironment that impact viral uptake.

Friedman and Lai [17] created a statistical framework to assess the effectiveness of oncolytic viruses in conjunction with checkpoint inhibitors, particularly anti-PD-1 anti-bodies, in cancer treatment. Using a system of partial differential equations, they simulate how immune cells, tumor cells, and oncolytic viruses interact. They found that therapy efficacy is not always improved by raising the inhibitor dosage. In some instances, the inhibitor may actually reduce the efficacy of the combination therapy for specific parameters. This finding emphasizes the importance of finding the precise correct dosage and regimen to optimize the effects of multiple treatments.

5.2 The Model

With the addition of virotherapy to our model from Chapter 4, we introduced two new equations. One represents the population dynamics of the virus. The other arises because the viruses injected into the tumor affect the cancer cells by infecting and disabling a fraction of them. We consider those cancer cells infected with the virus (K_I) and those not infected (K_U) as separate populations. This model allows us to study the effects of each treatment separately and also combinations of any or all of the three treatments.

The proposed model deals with the rate of change of the six variables as follows.

Model 5.2.1 (*Model for Chemotherapy, Immunotherapy and Virotherapy of a Cancer Tumor*). *Find four functions* $H, I, K_I, K_U, D, V : [0, T] \to \mathbb{R}^+$, *such that:*

$$\begin{aligned}
\frac{dH}{dt} &= \alpha_1 H(1 - \alpha_H H) - \gamma_1 K_U H - \mu_1 DH - \mu_H H, && (5.1)\\
\frac{dI}{dt} &= q + \psi + \alpha_2 I(1 - \alpha_I I) - \gamma_2 K_U I - \mu_2 DI - \mu_I I, && (5.2)\\
\frac{dK_I}{dt} &= \frac{\delta_1 K_U V}{\delta_2 + K_U} - \delta_3 K_I I - \delta_4 K_I D - \mu_{K_I} K_I, && (5.3)\\
\frac{dK_U}{dt} &= \alpha_3 K_U(1 - \alpha_{K_U}(K_I + K_U))\chi_1(K_U) - \frac{\delta_1 K_U V}{\delta_2 + K_U} - \gamma_3 K_U I\\
&- \mu_3 K_U D - \mu_{K_U} K_U, && (5.4)\\
\frac{dD}{dt} &= \varphi_D - \beta_1 ID - \beta_2 HD - \beta_3(K_U + K_I)D - \mu_D D, && (5.5)\\
\frac{dV}{dt} &= \varphi_V + \beta_4(\delta_3 I + \delta_4 D)K_I - \mu_V V. && (5.6)
\end{aligned}$$

Together with the initial conditions,

$$H(0) = H_0,\ I(0) = I_0,\ K_I(0) = K_{I0},\ K_U(0) = K_{U0},\ D(0) = D_0,\ V(0) = V_0. \tag{5.7}$$

As in the previous model, the rates are per day, the populations H, I, K_I, K_U are measured in the number of individuals, the units of D and V are arbitrary, and the various terms have the correct units.

The only change in equation (5.1), the equation for healthy cells in the system, as compared to the previous model is that $\gamma_1 KH$ becomes $\gamma_1 K_U H$ because infected cancer cells cannot attack other cells. The same is true for equation (5.2). The immune cells cannot be affected by the infected cancer cells, so $\gamma_2 KI$ becomes $\gamma_2 K_U I$, and this is the only difference between the equation for immune cells in this model, as compared to that in Chapter 4.

Equation (5.3) describes the rate of growth of tumor cells that have been infected by the virus. The growth rate, caused by infection, is assumed to be the

rate at which the uninfected tumor cells become infected $\frac{\delta_1 K_U V}{\delta_2 + K_U}$, where δ_1 denotes the growth rate constant and δ_2 a weight factor. The terms $\delta_3 K_I I$ and $\delta_4 K_I D$ are the rates at which the infected tumor cells are eliminated by the immune cells and the chemotherapy drug, respectively. The natural death rate constant for infected tumor cells is μ_{K_I}, which is likely to be very small.

Equation (5.4) describes the growth rate of active uninfected tumor cells, which threaten the health of the individual. The first component in this equation, $\alpha_3 K_U(1 - \alpha_{KU}(K_I + K_U))\chi_1(K_U)$, is a logistic growth term with a cutoff function, similar to that in (4.4). The growth rate constant, α_3, and the carrying capacity, $\frac{1}{\alpha_{K_U}}$, are applied to the sum of infected and uninfected cancer cells in the system, as both are utilizing resources. This term will go to zero when the uninfected cancer population is less than 1. The next term, $\frac{\delta_1 K_U V}{\delta_2 + K_U}$, is the rate of viral infection of the cancer cells, which is the term added to and described in equation (5.3). The loss of uninfected tumor cells due to interaction with immune cells and the chemotherapy drug are represented by γ_3 and μ_3, respectively. And the natural death rate constant of uninfected cancer cells is given by μ_{K_U} and is expected to be very small.

Equation (5.5) characterizes the dynamics of the chemotherapy drug in the system. The application rate of the drug is $\varphi_D = \varphi_D(t)$. This function represents the dosing regimen for a given treatment scenario. The terms $\beta_1 ID, \beta_2 HD$, and $\beta_3(K_U + K_I)$ represent the depletion rate of the drug as it interacts with immune, healthy, and all cancer cells, respectively. It is assumed that chemotherapy kills all cell types but at different rates. The natural depletion rate of the drug is μ_D.

Equation (5.6) is the rate equation for the virotherapy. The function $\varphi = \varphi(t)$ is the virotherapy treatment regimen. The term $\beta_4(\delta_3 I + \delta_4 D)K_I$ is included because it is assumed that when infected cancer cells are killed by immune

cells or the chemotherapy drug, the virus that they contained is released into the system. It is likely that δ_3 and δ_4 are very small. The factor β_4 is the average number of viruses released from a burst infected cell. The last term, $\mu_V V$, describes the loss of virus due to other causes.

We note that, while the chemotherapy drug and the virus are represented with their own equations, the immunotherapy treatment is a part of the immune cells equation because that seemed the natural way to consider them, just as we mentioned in Chapter 4.

The initial conditions for this model are set as follows to adhere to biological principles.

$$H(0) = H_0 \in (0, 1/\alpha_H),\ I(0) = I_0 > 0,\ K_I(0) = K_{I0} \geq 0,\ K_U(0) = K_{U0} > 0,$$

$$D(0) = D_0 \geq 0, \quad V(0) = V_0 \geq 0. \tag{5.8}$$

5.3 Analysis of the Model

We maintain the analysis structure from the previous model, with slight modifications for the addition of virotherapy. In this model, a chemotherapeutic drug, white platelets, and an infusion of modified viruses are eligible to be administered to the the tumor to eliminate it. The process of virotherapy is such that the viruses are injected into the tumor, and they affect the cancer cells by infecting and disabling a fraction of them.

For this model we must also show global solvability on every finite time interval by showing that if we start with nonnegative initial conditions, all solutions remain nonnegative and that every solution is bounded on every arbitrary finite time interval.

Proposition 5.3.1. Assume that the initial conditions satisfy (5.8) and q, φ_D, φ_V and ψ are Lipschitz, nonnegative and bounded functions, say $0 \leq q, \varphi_D, \varphi_V, \psi \leq M$. Then, every solution of system (5.1)–(5.6) satisfies the estimates:

$$0 < H \leq \frac{H_0 e^{\alpha_1 T}}{1 - \alpha_H H_0 + H_0 \alpha_H e^{\alpha_1 T}} \leq \frac{1}{\alpha_H}, \tag{5.9}$$

$$0 < I \leq \frac{\alpha_2 + \Delta}{2\alpha_2 \alpha_I}, \tag{5.10}$$

$$0 \leq K_I \leq K_{I0} + \frac{2A_*}{\mu_{K_I}}, \tag{5.11}$$

$$0 \leq K_U \leq \frac{K_{U0} e^{\alpha_3 T}}{(1 - \alpha_{K_U} K_{U0}) + K_{U0} \alpha_{K_U} e^{\alpha_3 T}} \leq \frac{1}{\alpha_{K_U}}, \tag{5.12}$$

$$0 \leq D \leq D_0 + \frac{2M}{\mu_D}, \tag{5.13}$$

$$0 \leq V \leq V_0 + \frac{2M}{\mu_V}, \tag{5.14}$$

for $0 < T < \infty$. Here,

$$C_* = M + \beta_4(\delta_3 + \delta_4)(C^*)^2, \tag{5.15}$$

$$A_* = \frac{\delta_1}{\delta_2}(C^*)^2. \tag{5.16}$$

We conclude that the *feasible region* Ω, that biologically makes sense, is

$$\Omega = \{(H, I, K_I, K_U, D, V) \in \mathbb{R}^6_+ :$$

$$H(t) \in \left(0, \frac{1}{\alpha_H}\right], \quad I(t) \in \left(0, \frac{\alpha_2 S + 1}{2\alpha_I S}\right], \quad K_I(t) \in \left[0, \frac{A_*}{\mu_{K_I}} + K_{I0}\right],$$

$$K_U(t) \in \left[0, \frac{1}{\alpha_{KU}}\right], \quad D(t) \in \left[0, \frac{M}{\mu_d} + D_0\right], \quad V(t) \in \left[0, \frac{C_*}{\mu_V} + V_0\right]\},$$

which is positively invariant for the system (5.1)–(5.6).

Proof. As in Chapter 4, we again begin by noting that the initial conditions are assumed to be positive. By the continuity of the solutions, there must exist some time interval $[0, t_0]$, $t_0 > 0$ on which the solutions remain nonnegative and bounded

by some positive constant C^*. The bounds for (5.1), (5.2), and (5.5) are identical to the bounds for (4.2), (4.3), and (4.5), respectively, where

$$\Delta = \sqrt{\alpha_2^2 + 8\alpha_2\alpha_I M}.$$

Estimate (5.4) is derived similarly to (4.4), when we note that

$$\alpha_3 K_U(1 - \alpha_{K_U}(K_I + K_U))\chi_1(K_U) \leq \alpha_3 K_U(1 - \alpha_{K_U} K_U).$$

The cutoff function χ_1 does not change the estimate.

To obtain (5.3) we proceed in the same way. Let $A_* = \dfrac{\delta_1 (C^*)^2}{\delta_2}$.

$$\frac{dK_I}{dt} \leq \frac{\delta_1 K_U V}{\delta_2 + K_U} - \mu_{K_I} K_I \leq A_* - \mu_{K_I} K_I.$$

Then

$$\left| K_I - \frac{A_*}{\mu_{K_I}} \right| \leq \left| K_{I0} - \frac{A_*}{\mu_{K_I}} \right| e^{-\mu_{K_I} t}.$$

Thus

$$K_I \leq K_{I0} + \frac{2A_*}{\mu_{K_I}}.$$

The bounds for V are comparable to those of D:

$$\frac{dV}{dt} \leq M + \beta_4(\delta_3 I + \delta_4 D)K_I - \mu_V V.$$

Letting $C_* = M + \beta_4(\delta_3 C^* + \delta_4 C^*)C^*$,

$$\frac{dV}{dt} \leq C_* - \mu_V V,$$

and so we have

$$V \leq \frac{C_*}{\mu_V} + \left| V_0 - \frac{C_*}{\mu_V} \right| e^{-\mu_V t} \leq V_0 + \frac{2C_*}{\mu_V}.$$

□

The system is Lipschitz on every arbitrary finite time interval, and globally bounded, which guarantees global existence.

Theorem 5.3.2 (Global Existence part 2)**.** *Assume that the initial conditions satisfy (5.8) and* q, ψ, φ_D, *and* φ_V *are smooth, positive and bounded functions. Then, system (5.1)–(5.6) has a unique smooth solution on every time interval* $[0, T]$, $0 < T < \infty$.

5.4 Stability

As in Chapter 4, to find the equilibrium points, we set the first order derivatives equal to zero. Again, finding these points is only of mathematical interest, since the purpose of the model is to find ways to drive the system to the DFE as quickly as possible. Let $(\bar{H}, \bar{I}, \bar{K}, \bar{D})$ denote the equilibrium values. The equilibrium system (omitting the bars) is as follows:

$$\begin{aligned}
0 &= \alpha_1 H(1-\alpha_H H) - \gamma_1 K_U H - \mu_1 DH - \mu_H H, \\
0 &= q + \psi + \alpha_2 I(1-\alpha_I I) - \gamma_2 K_U I - \mu_2 DI - \mu_I I, \\
0 &= \frac{\delta_1 K_U V}{\delta_2 + K_U} - \delta_3 K_I I - \delta_4 K_I D - \mu_{K_I} K_I, \\
0 &= \alpha_3 K_U(1-\alpha_{K_U}(K_I + K_U))\chi_1(K_U) - \frac{\delta_1 K_U V}{\delta_2 + K_U} - \gamma_3 K_U I \\
&- \mu_3 K_U D - \mu_{K_U} K_U, \qquad (5.17) \\
0 &= \varphi_D - \beta_1 ID - \beta_2 HD - \beta_3(K_U + K_I)D - \mu_D D, \\
0 &= \varphi_V + \beta_4(\delta_3 I + \delta_4 D)K_I - \mu_V V.
\end{aligned}$$

For biological reasons, we assume that the growth rate constants are larger than the death rate constants,

$$\alpha_1 > \mu_H, \qquad \alpha_2 > \mu_I. \qquad (5.18)$$

To study the stability of the equilibrium points, we compute the Jacobian matrix J of the system, given by:

$$J(H, I, K_I, K_U, D, V) =$$

$$\begin{bmatrix} J_{11} & 0 & 0 & -\gamma_1 H & -\mu_1 H & 0 \\ 0 & J_{22} & 0 & -\gamma_2 I & -\mu_2 I & 0 \\ 0 & -\delta_3 K_I & J_{33} & \frac{\delta_1\delta_2 V}{(\delta_2+K_U)^2} & -\delta_4 K_I & \frac{\delta_1 K_U}{\delta_2+K_U} \\ 0 & -\gamma_3 K_U & -\alpha_3\alpha_{K_U} K_U\chi_1 & J_{44} & -\mu_3 K_U & -\frac{\delta_1 K_U}{\delta_2+K_U} \\ -\beta_2 D & -\beta_1 D & -\beta_3 D & -\beta_3 D & J_{55} & 0 \\ 0 & \beta_4\delta_3 K_I & \beta_4\delta_3 I + \beta_4\delta_4 D & 0 & \beta_4\delta_4 K_I & -\mu_V \end{bmatrix}, \tag{5.19}$$

where the terms $J_{11} - J_{55}$ are given by:

$$\begin{aligned} J_{11} &= \alpha_1(1 - 2\alpha_H H) - \gamma_1 K_U - \mu_1 D - \mu_H, \\ J_{22} &= \alpha_2(1 - 2\alpha_I I) - \gamma_2 K_U - \mu_2 D - \mu_I, \\ J_{33} &= -\delta_3 I - \delta_4 D - \mu_{KI}, \\ J_{44} &= (\alpha_3 - \alpha_3\alpha_{KU} K_I - 2\alpha_3\alpha_{KU} K_U)\chi_1 - \frac{\delta_1\delta_2 V}{(\delta_2 + K_U)^2} - \gamma_3 I - \mu_3 D - \mu_{KU}, \\ J_{55} &= -\beta_2 H - \beta_1 I - \beta_3(K_I + K_U) - \mu_D. \end{aligned}$$

5.4.1 Disease-Free Equilibrium

First, we study the DFE and observe that in such a case we need to have $K_I = K_U = 0$ and $\psi = \varphi_D = \varphi_V = 0$, hence $D = V = 0$, since neither drug nor virotherapy is needed. Moreover, q is a positive constant. Thus, the system reduces, as it did in Chapter 4, to the two equations:

$$\alpha_1 H(1 - \alpha_H H) - \mu_H H = 0,$$

$$q + \alpha_2 I(1 - \alpha_I I) - \mu_I I = 0.$$

Thus, the only feasible solution is

$$\left(\frac{\alpha_1 - \mu_H}{\alpha_1 \alpha_H}, \frac{(\alpha_2 - \mu_I) + \sqrt{(\alpha_2 - \mu_I)^2 + 4\alpha_2 \alpha_I q}}{2\alpha_2 \alpha_I}, 0, 0, 0, 0 \right). \tag{5.20}$$

In the numerical simulations, in the case of convergence to a DFE, we have

$$(H, I) = (9.5 \times 10^7, 1.4 \times 10^7).$$

Then, in the DFE, we have

$$J(H, I, 0, 0, 0, 0) = \begin{bmatrix} J_{11} & 0 & 0 & -\gamma_1 H & -\mu_1 H & 0 \\ 0 & J_{22} & 0 & -\gamma_2 I & -\mu_2 I & 0 \\ 0 & 0 & J_{33} & 0 & 0 & 0 \\ 0 & 0 & 0 & J_{44} & 0 & 0 \\ 0 & 0 & 0 & 0 & J_{55} & 0 \\ 0 & 0 & J_{63} & 0 & 0 & -\mu_V \end{bmatrix}. \tag{5.21}$$

Here, we used the fact that $\chi_1(0) = 0$, and

$$J_{11} = (\alpha_1 - \mu_H) - 2\alpha_1 \alpha_H H = -(\alpha_1 - \mu_H) < 0,$$

$$J_{22} = (\alpha_2 - \mu_I) - 2\alpha_2 \alpha_I I = -\sqrt{(\alpha_2 - \mu_I)^2 + 4\alpha_2 \alpha_I q} < 0,$$

$$J_{33} = -\delta_3 I - \mu_{KI} = -\delta_3 \left(\frac{(\alpha_2 - \mu_I) + \sqrt{(\alpha_2 - \mu_I)^2 + 4\alpha_2 \alpha_I q}}{2\alpha_2 \alpha_I} \right) - \mu_{KI} < 0,$$

$$J_{44} = -\gamma_3 I - \mu_{KU} = -\gamma_3 \left(\frac{(\alpha_2 - \mu_I) + \sqrt{(\alpha_2 - \mu_I)^2 + 4\alpha_2 \alpha_I q}}{2\alpha_2 \alpha_I} \right) - \mu_{KU} < 0,$$

$$J_{55} = -\beta_2 H - \beta_1 I - \mu_D = -\beta_1 \left(\frac{(\alpha_2 - \mu_I) + \sqrt{(\alpha_2 - \mu_I)^2 + 4\alpha_2 \alpha_I q}}{2\alpha_2 \alpha_I} \right)$$
$$-\beta_2 \frac{(\alpha_1 - \mu_H)}{\alpha_1 \alpha_H} - \mu_D < 0,$$

$$J_{63} = \beta_4 \delta_3 I = \beta_4 \delta_3 \left(\frac{(\alpha_2 - \mu_I) + \sqrt{(\alpha_2 - \mu_I)^2 + 4\alpha_2 \alpha_I q}}{2\alpha_2 \alpha_I} \right) > 0.$$

It is seen that all the terms on the main diagonal are negative, and so are all the terms above the main diagonal. Using Mathematica, we find that the eigenvalues are

$$\lambda_1 = J_{11}, \;\; \lambda_2 = J_{22}, \;\; \lambda_3 = J_{33}, \;\; \lambda_4 = J_{44}, \;\; \lambda_5 = J_{55}, \;\; \lambda_6 = -\mu_V. \tag{5.22}$$

Since all the eigenvalues are negative, we conclude,

Proposition 5.4.1. The Disease Free Equilibrium in model (5.17) is stable and attracting.

However, as was noted above, our interest is in reaching the disease-free state as fast as possible, and not just waiting until cancer vanishes on its own, which may take a very long time.

5.4.2 Endemic equilibrium

To obtain the EE states, we need to solve the full system (5.17), with $\chi_1 = 1$. However, our main interest in this work is in the eradication of cancer cells. Hence, the EE are only of mathematical interest. For the sake of completeness, we describe the stability of the EE in the appendix of this chapter, Section 5.7 .

5.5 Simulations

First, we consider the system without any treatment. Using the parameter values in Table 5.1 together with the initial values $H_0 = 10^6$, $I_0 = 10^3$, $K_{I0} = 0$, $K_{U0} = 10^5$, $D_0 = 0$ and $V_0 = 0$, leads to the results depicted in Figure 5.1. We separated the 'No Treatment' scenario into two graphs to better illustrate the behavior of healthy and immune cells, since their populations are significantly smaller than those of cancer cells. In the presence of cancer, and without treatment, the cancer increases to its carrying capacity of $K_U = 9.7$ x 10^9 in about 35 days, see Figure 5.1(L). The behavior of the healthy and immune cells is shown in Figure 5.1(R). Both of these populations grow some and then rapidly decline to zero. The model predicts the spread of cancer to its maximum possible extent and the extinction of the healthy and immune cells before that.

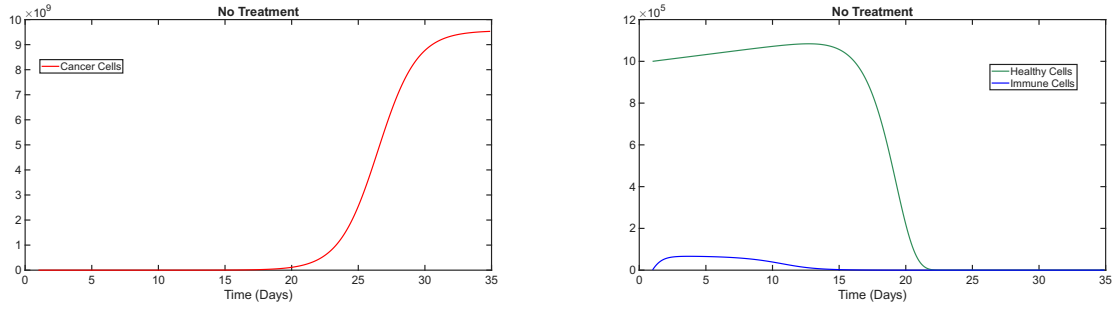

Figure 5.1: No Treatment. The behavior of the cancer cells without any treatment (L) and the behavior of healthy and immune cells (R). Data values are shown in Table 5.1. Healthy and immune cells decline as the cancer grows, and without treatment, these cells eventually die out completely while cancer grows until it reaches its carrying capacity in about 35 days. Note the different scales.

Table 5.1: Symbols and the values of the baseline parameters

Parameter	Value	Description
q	10^5	rate of supply of immune cells
α_1	0.01	maximal growth rate constant of healthy cells
α_2	0.024	maximal growth rate constant of immune cells
α_3	0.693	maximal growth rate constant of tumor cells
α_H	10^{-8}	reciprocal of healthy cell carrying capacity
α_I	$2\text{x}10^{-8}$	reciprocal of immune cell carrying capacity
α_{KU}	$1.03\text{x}10^{-10}$	reciprocal of uninfected cell carrying capacity
γ_1	10^{-8}	loss rate of healthy cells due to uninfected tumor cells
γ_2	10^{-5}	loss rate of immune cells due to uninfected tumor cells
γ_3	10^{-5}	loss rate of uninfected cancer cells due to immune cells
μ_1	0.1	death rate of healthy cells due to drug
μ_2	0.2	rate at which the drug kills immune cells
μ_3	0.3	death rate of uninfected cancer cells due to drug
μ_H	0.0005	natural mortality rate of healthy cells
μ_I	0.024	natural death rate of immune cells
μ_{KI}	3.66	natural death rate of infected immune cells
μ_{KU}	0.01	natural death rate of uninfected cancer cells
μ_D	1.5	natural decay in vivo of the drug
μ_V	1	natural decay rate constant of viruses
δ_1	0.054	rate constant of infection of cancer by virus
δ_2	200	weight factor
δ_3	0.027	death rate of infected cancer due to immune cells

Table Continued on Next Page

Table 5.1: Symbols and the values of the baseline parameters

Parameter	Value	Description
	Table Continued from Previous Page	
δ_4	0.0178	death rate of infected cancer due to drug
β_1	10^{-10}	drug decrease rate due to immune cells
β_2	10^{-10}	drug decrease rate due to cancer cells
β_3	10^{-10}	drug decrease constant due to normal cells
β_4	50.8	multiplier of viruses created by infected cells

Next, we consider each treatment on its own. We apply chemotherapy once a week with dose $\varphi_D = 1.6$. Figure 5.2 shows that in this case cancer is eliminated around day 29, after three chemotherapy treatments. Once cancer is eliminated the treatment is discontinued. The healthy and immune cells then grow to reach their steady state values, $H = 9.5 \times 10^7$ and $I = 1.4 \times 10^7$, indicating a complete recovery from the disease.

Figure 5.3 shows the simulations when only immunotherapy is applied. The dose of immunotherapy is represented in the system as ψ, and we use $\psi = 41,489$. This treatment is applied once every three weeks. The results indicate that cancer is eradicated around day 57, after three immunotherapy treatments. Another visible aspect of the immunotherapy simulation is that healthy cells are not noticeably affected by the cancer or the treatment in this case.

We complete the set of single treatments with virotherapy, represented in the system as φ_V. It is applied once a week and is set as $\varphi_V = 10$. Figure 5.4 shows that the cancer disappears around day 17, after only two virotherapy treatments. The behavior of this simulation is very different from the other two treatments in

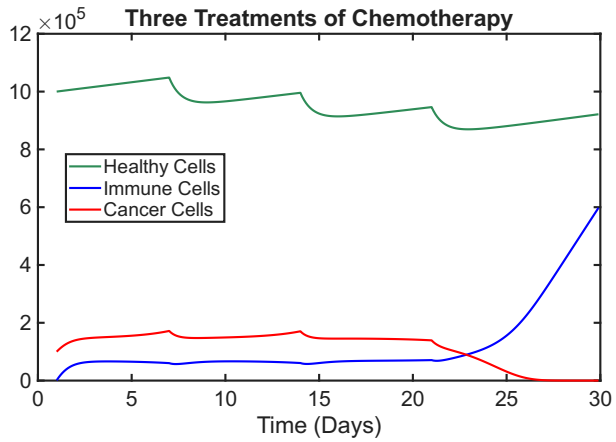

Figure 5.2: Chemotherapy. Chemotherapy is applied in a weekly dose of $\varphi_D = 1.6$ on days 7, 14, and 21. It is seen that after three rounds of chemotherapy cancer is eliminated on day 29. The effect of chemotherapy on the healthy cells is noticeable, in addition to killing cancer cells. Eventually the healthy and immune cells reach their steady state values.

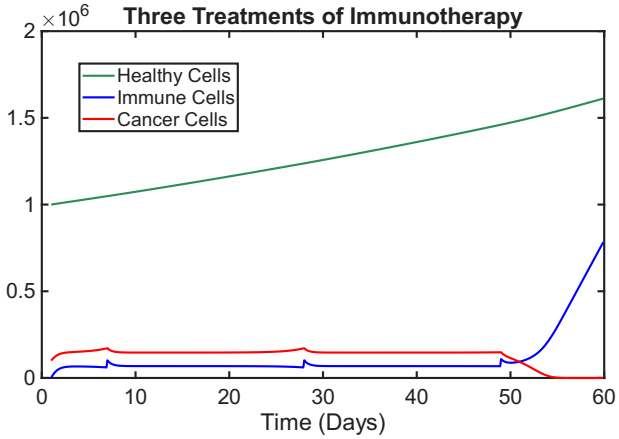

Figure 5.3: Immunotherapy. The therapy is applied every three weeks and $\psi = 41,489$. This treatment is given on days 7, 28, and 49. Following three rounds of immunotherapy, the cancer is eliminated on day 57. The healthy cells are not affected by the therapy.

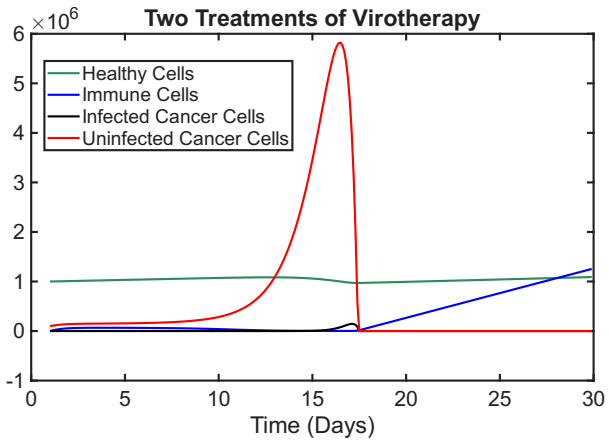

Figure 5.4: Virotherapy. The treatment is applied in a weekly dose of $\varphi_V = 10$ on days 7 and 14. After two rounds of virotherapy, cancer disappears on day 17.

that the cancer grows to a much higher level before dropping off at a very steep rate and vanishing.

With these three separate individual treatment simulations established, we seek to test different combinations of treatments in an effort to maximize the effectiveness, i.e. the quickest elimination of the cancer. To this end, we investigate four different possible scenarios and the results predicted by the model.

5.5.1 Combinations of Treatments

We now turn to the main purpose of the model, which is to find better outcomes by using combinations of treatments. To that end, we consider the following computer experiments. We apply all three treatments together each week for a few weeks. This simultaneous application eradicates cancer faster than any single treatment. This scenario is chosen to analyze and show the predictions of the system. We do not know if it is a probable treatment schedule, as this may be too much for the patient's system to handle.

We keep the treatment levels the same as is done for each treatment type applied individually:

$$\varphi_D = 1.6, \qquad \psi = 41,489, \qquad \varphi_V = 10.$$

The simulation results are shown in Figure 5.5. After a single treatment of all three therapies on the same day, the cancer vanishes on day 14.

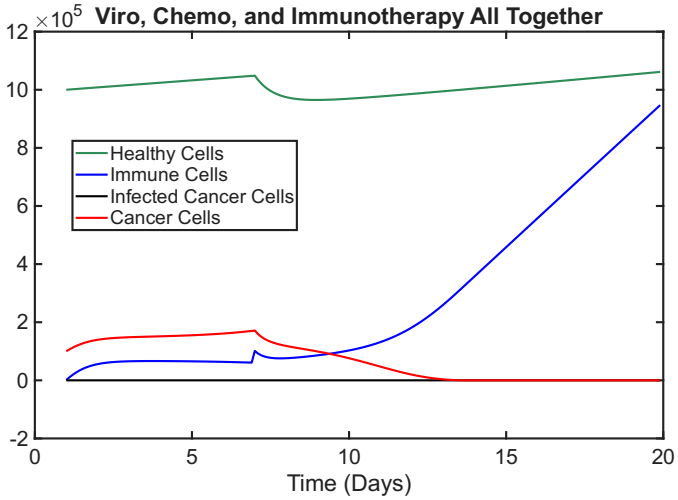

Figure 5.5: Three Treatments at once. All three therapies are applied on day 7 as a test of the model predictions. Cancer is eradicated on day 14, much sooner than in any individual or combination treatment.

To gain further insight into the model predictions, we run simulations in which we apply the treatments in a cycle of seven-day intervals. We use the same constants as given in Table 5.1. Figure 5.6 shows the case where chemotherapy treatment is applied on day 7, followed by immunotherapy on day 14. The

application of virotherapy on day 21 is not required, as the cancer vanishes by day 28 without it.

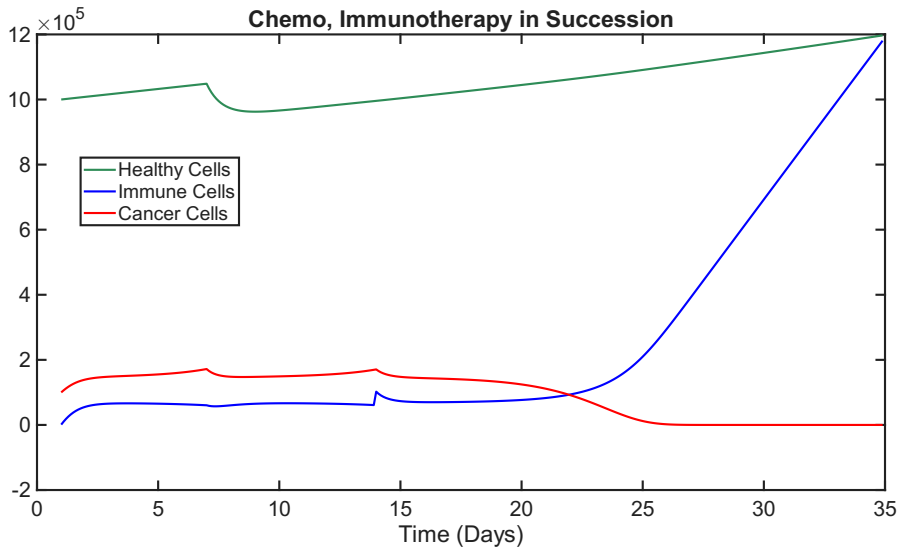

Figure 5.6: Two Treatments in Succession. Chemotherapy administered on day 7 and immunotherapy on day 14. Cancer vanishes ($K_U < 1$) after the first round of treatments, on day 28. Then, the healthy and immune cell populations increase monotonically towards their steady states.

Figure 5.7 shows the results of intending to apply immunotherapy on day 7, chemotherapy on day 14, and virotherapy on day 21 in succession. It is found that the cancer is gone by day 22 and, therefore, there was no need for the virotherapy treatment. Similarly, in Figure 5.8, we simulate the treatment of immunotherapy on day 7, virotherapy on day 14, and chemotherapy on day 21. Again, the third treatment was not required to eliminate the cancer, since it was gone by day 21.

When assessing the benefits of a treatment schedule, there is more to consider than the amount of time needed to eradicate the cancer. If we compare

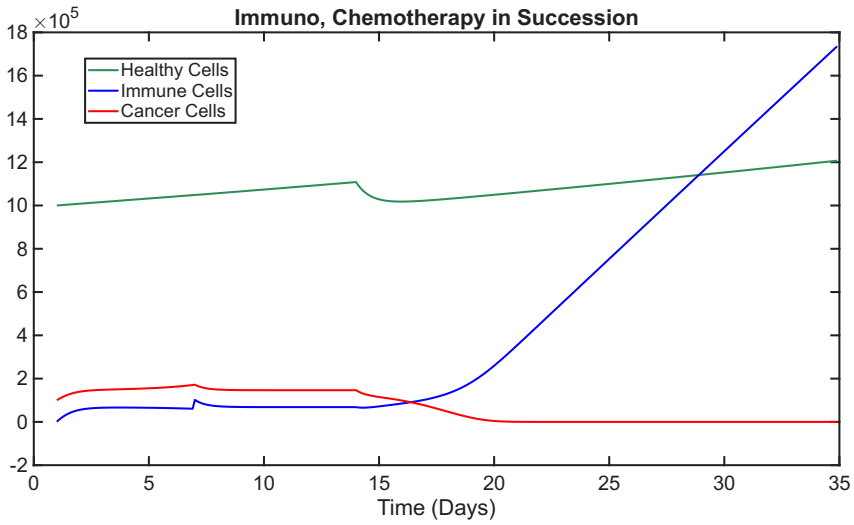

Figure 5.7: Two Treatments in Succession. Treatments administered weekly, alternating among immunotherapy, chemotherapy, and virotherapy. Cancer (red – uninfected cells) vanishes ($K_U < 1$) after the first two treatments, on day 22, so the virotherapy was not required.

Figure 5.7 to Figure 5.8, we see that they both eliminate cancer in roughly the same amount of time. However, the cancer begins to decrease about seven days sooner in the Immuno, Chemo combination, as compared to the Immuno, Viro combination. Such details may be of interest when comparing treatment regimens.

In other experiments with different combinations of the three treatments, but with the same treatment amounts, we obtained very similar results, in which the cancer vanished between 20 and 29 days.

We note that many of the system coefficients are arbitrary, not based on data, and that the disappearance of the cancer in two or three weeks is the model's artifact. However, if medically safe, these results indicate that combinations of treatments may be more effective than each one separately.

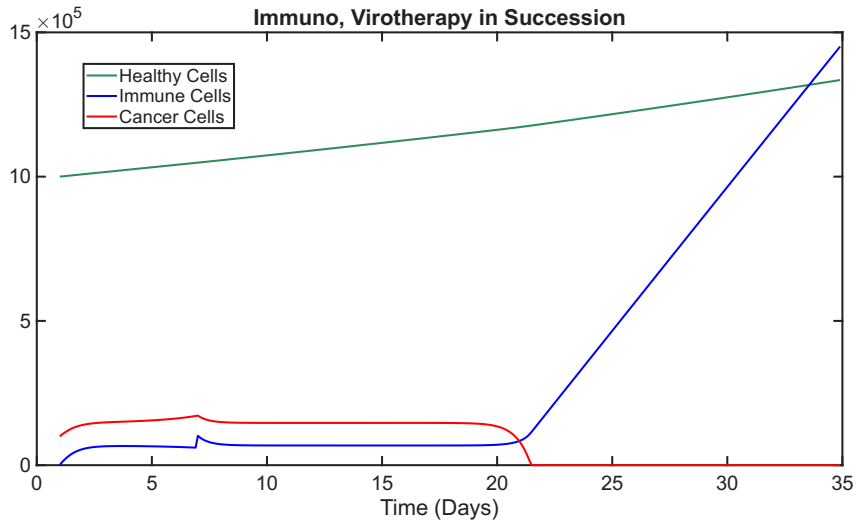

Figure 5.8: Two Treatments in Succession. Treatments administered weekly, alternating among immunotherapy, virotherapy, and chemotherapy. Cancer vanishes ($K_U < 1$) after the first two treatments, on day 21, so chemotherapy was not required.

5.6 Conclusions and future work

As in Chapter 4, our results indicate that combined therapies may be more effective than a single therapy. Our next step is to validate both models with data and use those results to optimize treatment scheduling among chemotherapy, immunotherapy, and virotherapy. Other future work includes performing parameter sensitivity analysis to find out which are the important parameters, adding randomness to the system, and studying the attractors in the system to find if the model supports chaos. We believe that the model and its variants will find ways to be applied in real world cancer treatments.

5.7 Stability of endemic equilibrium

As noted in Section 5.4.2, we present the study of the endemic equilibrium (EE) here. However, since the DFE is stable and attracting, we expect the EE to be

unstable. We use the Jacobian matrix (5.24). Let $(H^*, I^*, K_I^*, K_U^*, D^*, V^*)$ be the EE point. We are interested in the case when $K_U \geq 1$, hence $\chi_1(K_U) = 1$. Moreover, in the EE state, there are no interventions, hence $\psi = \varphi_D = \varphi_V = 0$. Then, the system is (5.17),

The equilibrium system (omitting the stars), is the following:

$$\begin{aligned}
0 &= \alpha_1 H(1-\alpha_H H) - \gamma_1 K_U H - \mu_1 D H - \mu_H H, \\
0 &= q + \alpha_2 I(1-\alpha_I I) - \gamma_2 K_U I - \mu_2 D I - \mu_I I, \\
0 &= \frac{\delta_1 K_U V}{\delta_2 + K_U} - \delta_3 K_I I - \delta_4 K_I D - \mu_{K_I} K_I, \\
0 &= \alpha_3 K_U(1-\alpha_{K_U}(K_I + K_U)) - \frac{\delta_1 K_U V}{\delta_2 + K_U} - \gamma_3 K_U I \\
&- \mu_3 K_U D - \mu_{K_U} K_U, \\
0 &= -\beta_1 I D - \beta_2 H D - \beta_3 (K_U + K_I) D - \mu_D D, \\
0 &= \beta_4(\delta_3 I + \delta_4 D) K_I - \mu_V V.
\end{aligned} \tag{5.23}$$

Next, the Jacobian matrix at the EE (stars omitted) is

$$J(H, I, K_I, K_U, D, V) =$$

$$\begin{bmatrix}
J_{11} & 0 & 0 & -\gamma_1 H & -\mu_1 H & 0 \\
0 & J_{22} & 0 & -\gamma_2 I & -\mu_2 I & 0 \\
0 & -\delta_3 K_I & J_{33} & \frac{\delta_1 \delta_2 V}{(\delta_2 + K_U)^2} & -\delta_4 K_I & \frac{\delta_1 K_U}{\delta_2 + K_U} \\
0 & -\gamma_3 K_U & -\alpha_3 \alpha_{K_U} K_U & J_{44} & -\mu_3 K_U & -\frac{\delta_1 K_U}{\delta_2 + K_U} \\
-\beta_2 D & -\beta_1 D & -\beta_3 D & -\beta_3 D & J_{55} & 0 \\
0 & \beta_4 \delta_3 K_I, & \beta_4 \delta_3 I + \beta_4 \delta_4 D & 0 & \beta_4 \delta_4 K_I & -\mu_V
\end{bmatrix}, \tag{5.24}$$

where the terms $J_{11} - J_{55}$ are given by:

$$\begin{aligned}
J_{11} &= \alpha_1(1 - 2\alpha_H H) - \gamma_1 K_U - \mu_1 D - \mu_H, \\
J_{22} &= \alpha_2(1 - 2\alpha_I I) - \gamma_2 K_U - \mu_2 D - \mu_I, \\
J_{33} &= -\delta_3 I - \delta_4 D - \mu_{KI}, \\
J_{44} &= (\alpha_3 - \alpha_3\alpha_{KU} K_I - 2\alpha_3\alpha_{KU} K_U) - \frac{\delta_1\delta_2 V}{(\delta_2 + K_I)^2} - \gamma_3 I - \mu_3 D - \mu_{KU}, \\
J_{55} &= -\beta_2 H - \beta_1 I - \beta_3(K_I + K_U) - \mu_D.
\end{aligned}$$

The characteristic equation is

$$\lambda^6 + M_1\lambda^5 + M_2\lambda^4 + M_3\lambda^3 + M_4\lambda^2 + M_5\lambda + M_6 = 0, \tag{5.25}$$

where,

$M_1 = -\text{Trace}(J) = -(J_{11} + J_{22} + J_{33} + J_{44} + J_{55} + J_{66})$,

M_2 is the sum of all principal 2×2 minors of J,

$-M_3$ is the sum of all principal 3×3 minors of J,

M_4 is the sum of all principal 4×4 minors of J,

$-M_5$ is the sum of all principal 5×5 minors of J,

$M_6 = Det(-J)$.

Now, we apply the Routh-Hurwitz criteria to find the stability conditions of the characteristics equation. Routh-Array:

λ^6	1	M_2	M_4	M_6
λ^5	M_1	M_3	M_5	0
λ^4	$b_1 = \frac{M_1 M_2 - M_3}{M_1}$	$b_2 = \frac{M_1 M_4 - M_3}{M_1}$	M_6	0
λ^3	$c_1 = \frac{b_1 M_3 - M_1 b_2}{b_1}$	$c_1 = \frac{b_1 M_5 - M_1 M_6}{b_1}$	0	0
λ^2	$d_1 = \frac{c_1 b_2 - b_1 c_2}{c_1}$	M_6	0	0
λ^1	$e_1 = d_1 c_2 - c_1 d_2$	0	0	0
λ^0	M_6	0	0	0

According to the Routh criterion, the first column must all be positive, that is,

$$
\begin{aligned}
&M_1 > 0, \\
&b_1 = \frac{M_1 M_2 - M_3}{M_1} > 0, \\
&c_1 = \frac{b_1 M_3 - M_1 b_2}{b_1} > 0, \\
&d_1 = \frac{c_1 b_2 - b_1 c_2}{c_1} > 0, \\
&e_1 = \frac{d_1 c_2 - c_1 M_6}{d_1} > 0, \\
&M_6 > 0.
\end{aligned}
$$

We conclude that when all six conditions are satisfied, the EE is asymptotically stable. If one of the conditions is reversed, the system remains unstable.

CHAPTER SIX

Conclusions

Within the three models in this dissertation, we have established that the populations in the models are positive, invariant, and bounded, and the solutions to the models exist. We have assessed the conditions for stability and approximated the solutions using numerical methods, which we plotted to better understand the behavior of the system. These three models were constructed to gain insight and help improve the understanding of complicated biological processes involved in the spread of disease.

Our modified SIR model is based on the original SIR model established by Kermack and McKendrick. Their model has been extensively studied through the years. One of the most attractive qualities of these models is their simplicity. One of the primary challenges is to create a SIR model that more accurately reflects the dynamics of the spread of disease, while maintaining a form simple enough to be analyzed. With what we observed in the COVID-19 epidemic, the varying infection rate and varying hospitalization rate were significant aspects of the disease spread. We developed our model to address these aspects of diseases in general, not just for COVID-19. Within our model, we identified conditions under which we approach a disease-free equilibrium, so that the disease is eventually eliminated, and conditions that lead to an endemic equilibrium, so that the disease persists in the population. We confirmed these findings through our simulations. We also shared a scenario where we manipulated the infectivity of the disease to illustrate the response of the system. In this case, the change in β affected all of the variables in the short term, but the solution converged to the same EE limit as the simulation with no change in

β. From our results, several topics of further study have arisen. In particular, how do we find the functional forms of Ψ_β and Ψ_* for a given disease? Can we find initial conditions that are guaranteed to converge to any specified steady state, given that each choice of β_S and α_S corresponds to one steady state, creating a continuum of steady states within the model? What effect will it have to add randomness or periodicity to some of the system coefficients to better simulate new disease variants, since simply adding random impulses to the equations for β and α^* did not have a lasting effect?

As for cancer treatment, it is becoming more common to consider combining cancer treatments [30], [32], [36], [40]. For our first combination cancer treatment model, we consider the combination of chemotherapy and immunotherapy. After developing and analyzing the model and looking into current treatments in more detail, we decided to create a more complex model that also includes virotherapy. The addition of two equations to our original system created an added layer of complexity, while still providing expected results, namely that all treatments given together are mathematically most effective and combinations of therapies may lead to a more efficient elimination of the tumor. For future work on both of these models, we plan to apply the models to established data, determine the parameter values that reflect the observed behavior of the system, and test them in different treatment schedules in search of patterns and best practices.

The three models presented here offer fresh insights into the field of mathematical epidemiology. They build upon the fundamentals of such types of models. We have developed a framework to better understand the effects of an evolving disease on a population and have also created two methods to assess the effectiveness of combination cancer treatments. These are two areas that have a

profound impact on human health. It is our hope that these models will be instructive on best practices for mitigating the effects of cancer and other diseases.

REFERENCES

[1] A.L.Hodgkin and A.F.Huxley, *A quantitative description of membrane current and its application to conduction and excitation in the nerve*, J.Physiol. (1952).

[2] J.P. Allison and T. Honjo, *Cancer immunotherapy: Co-stimulatory agonists and co-inhibitory antagonists*, AIMS Mathematics (2009).

[3] A.M.Turing, *The chemical basis of morphogenesis*, Phil.Trans.R.Soc.Lond. (1952).

[4] William E. Boyce and Richard C. DiPrima, *Elementary differential equations and boundary value problems*, sixth ed., p. 339, John Wiley And Sons, Inc, 1997.

[5] F. Brauer, *Mathematical epidemiology: Past, present, and future*, Infect. Dis. Model (2017).

[6] Tomás Caraballo and Xiaoying Han, *Applied nonautonomous and random dyanamical systems*, pp. 4–5, Springer, 2016.

[7] A. Cesmelioglu, K. L. Kuttler, M. Shillor, and A. M. Spagnuolo, *A mathematical model of the COVID-19 pandemic dynamics with dependent variable infection rate: Application to the Republic of Korea*, arXiv:2008.03248 (2021).

[8] Tomas B. Co, *Runge kutta method for solving ode*, 2018.

[9] A. Das, K. Dehingial, Hemanta Kumar Sarmah, C. Park, Jung Rye Lee, K. Sadri, and K. Hosseini, *Optimal control of effector-tumor-normal cells dynamics in presence of adoptive immunotherapy*, AIMS Mathematics (2021).

[10] A. Das, R. Paul, K. Dehingia, and Hemanta Kumar Sarmah, *An analysis of the dynamics of a cancerous tumour model with targeted chemotherapy*, Asian Journal of Pharmaceutical Research and Health Care (2020).

[11] L.G. de Pillis, K.R. Fister, W. Gu, Tiffany Head, Kenny Maples, Todd Neal, Anand Murugan, and Kenji Kozai, *Optimal control of mixed immunotherapy and chemotherapy of tumors*, Journal of Biological Systems (2008).

[12] L.G. de Pillis, W. Gua, and A.E. Radunskaya, *Mixed immunotherapy and chemotherapy of tumors: modeling, applications and biological interpretations*, J. Theoretical Biology (2006).

[13] O. Diekman, J.A.P. Heesterbeek, and M.G. Roberts, *The construction of next-generation matrices for compartmental epidemic models*, J.Roy. Soc. Interface (2010).

[14] Tarini Kumar Dutta, Silmera Sangma, Janice Moore, and Meir Shillor, *A mathematical model for chemotherapy, immunotherapy and virotherapy treatments of cancer*, arXiv:2602.23488v1 (2026).

[15] Tarini Kumar Dutta, Meir Shillor, Janice Moore, and Silmera A. Sangma, *A model for cancer chemo-immunotherapy treatment schedules*, BIOMATH (2025).

[16] F. Frascoli, P.S. Kim, B.D. Hughes, and K.A. Landman, *A dynamical model of tumour immunotherapy*, Mathematical Biosciences (2014).

[17] A. Friedman and X. Lai, *Combination therapy for cancer with oncolytic virus and checkpoint inhibitor: A mathematical model*, PLOS One (2018).

[18] Stephen W. Goode and Scott A. Annin, *Differential equations and linear algebra*, Pearson, 2017.

[19] Herbert W. Hethcote, *The mathematics of infectious diseases*, SIAM Review (2000).

[20] Morris W. Hirsch, Stephen Smale, and Robert L. Devaney, *Differential equations, dynamical systems and an introduction to chaos*, second ed., p. 397, Elsevier, 2004.

[21] F.S. E. J. Shi, O. Alagoz and Q. Su, *A survey of optimization models on cancer chemotherapy treatment planning*, Ann. Oper. Res. (2014).

[22] William Ogilvy Kermack and A.G.McKendrick, *A contribution to the mathematical theory of epidemics*, Proceedings A (1927).

[23] P.E. Kloeden and M. Rasmussen, *Nonautonomous dynamical systems*, Mathematical Surveys and Monographs (2011).

[24] S.A. Levin, *The problem of pattern and scale in ecology*, Ecology (1992).

[25] ———, *Frontiers in mathematical biology*, Springer, 1994.

[26] J. Moore and M. Shillor, *A modified sir model with dependent infection and hospitalization rates*, BIOMATH (20241).

[27] J.D. Murray, *A simple method for obtaining approximate solutions for a class of diffusion-kinetic enzyme problems*, Math.Biosci. (1968).

[28] ———, *Mathematical biology, i: An introduction*, Springer, 2000.

[29] ———, *Vignettes from the field of mathematical biology: the application of mathematics to biology and medicine*, Interface Focus (2012).

[30] Farshac Nassiri, Vikas Patil, Leeor S Yefet, and Olivia Singh, *Oncolytic dnx-2401 virotherapy plus pembrolizumab in recurrent glioblastoma: a phase 1/2 trial*, Nature Medicine (2023).

[31] O. Nava, *A mathematical model for treatment using chemo-immunotherapy*, Heliyon (2022).

[32] Andrew Nguyen, Louisa Ho, and Yonghong Wan, *Chemotherapy and oncolytic virotherapy: Advanced tactics in the war against cancer*, Frontiers in Oncology (2014).

[33] Nomenclature Committee of the International Union of Biochemistry, *Symbolism and terminology in enzyme kinetics*, European Journal of Biochemistry (1981).

[34] L. Pang, L. Shen, and Z. Zhao, *Mathematical modelling and analysis of the tumor treatment regimens with pulsed immunotherapy and chemotherapy*, Computational and Mathematical Methods in Medicine (2016).

[35] P. Pooladvand, C.–Ok Yun, A. Rum Yoon, P. S. Kim, and F. Frascoli, *The role of viral infectivity in oncolytic virotherapy outcomes : A mathematical study*, Mathematical Biosciences (2021).

[36] Masmudur M. Rahman and Grant McFadden, *Oncolytic viruses: Newest frontier for cancer immunotherapy*, Cancers (2021).

[37] D.S. Rodrigues, P.F.A. Mancera, T. Carvalho, and L.F. Gonçalves, *A mathematical model for chemo-immunotherapy of chronic lymphocytic leukemia*, Applied Mathematics and Computation (2019).

[38] H. Schättler and U. Ledzewicz, *Optimal control for mathematical models of cancer therapies, an application of geometric methods*, Springer, 2015.

[39] G. Song, *Mathematical modeling and analysis of tumor chemotherapy*, Symmetry (2022).

[40] Christian Sordo-Bahamonde, Seila Lorenzo-Herrero, Ana P. Martinez-Perez, Juan Rodrigo, Juana Garcia-Pedrero, and Segundo Gonzalez, *Chemo-immunotherapy: A new trend in cancer treatment*, Cancers (2023).

[41] D. Wodarz and N. Komarova, *Towards predictive computational models of oncolytic virus therapy: basis for experimental validation and model selection*, PLOS One (2009).